GEOCHEMISTRY OF EYJAFJÖLL
A VOLCANO IN SOUTHERN ICELAND

by

BARBARA HOLOTA ARNEY

B.S., Boston College
(1974)

SUBMITTED IN PARTIAL FULFILLMENT
OF THE REQUIREMENTS FOR THE
DEGREE OF

MASTER OF SCIENCE

at the

MASSACHUSETTS INSTITUTE OF TECHNOLOGY

(May 1978)

GEOCHEMISTRY OF EYJAFJÖLL
A VOLCANO IN SOUTHERN ICELAND

by

BARBARA HOLOTA ARNEY

Submitted to the Department of Earth and Planetary Sciences on 19 May 1978 in partial fulfillment of the requirements for the Degree of Master of Science.

ABSTRACT

Major element whole rock analyses of samples from the volcano Eyjafjöll and compositions of selected phenocryst phases within them have been used to develop a fractionation model relating the various rock types produced by the volcano. Considerable subtraction of olivine from a hypothetical primary magma is required to produce even the least silicic compositions observed at the surface. More silicic compositions can be derived from one of two "parent" compositions, chosen from the least differentiated rocks sampled, by further subtraction primarily of plagioclase, clinopyroxene, and magnetite with minor ilmenite and olivine. No separate source or mechanism is required to produce the small quantities of rhyolite found, as they can be derived by fractionation. There is some evidence that the magmas of Eyjafjöll have become less alkalic and more silica saturated with time.

Thesis Supervisor: John S. Dickey, Jr.
Title: Associate Professor of Geology

TABLE OF CONTENTS

LIST OF FIGURES

LIST OF TABLES

INTRODUCTION

Eyjafjöll is a central volcano in southern Iceland. Located in the eastern neo-volcanic zone, it is the volcano nearest the coast, in line with Heimaey and Surtsey offshore. From Eyjafjöll the eastern neo-volcanic zone continues northeast through Eldgja, Laki, and Askja before turning north (Fig. 1). Directly north of Eyjafjöll are Tindalfjall and Hekla. Hekla is approximately 37 km north of Eyjafjöll; Heimaey is approximately 25 km to the southwest. Katla, under Myrdalsjokull, is directly east of Eyjafjöll.

In his discussion of recent basalts in Iceland, Jakobsson (1972) classes Eyjafjöll, Katla, Hekla, and Eldgja as transitional alkali, while Heimaey and Surtsey are alkali basalt. Most of the neo-volcanic basalts are tholeiites. The division into alkali vs. transitional seems to have been based on the CPIW norms, the transitional alkali having neither nepheline nor quartz, much more olivine, and very much less hypersthene than the tholeiites. Alkali basalts are nepheline normative.

This volcano was chosen for study because of its location on the coast, at the edge of the transitional alkali zone. (Hekla has been much studied, and the tephras of Katla, which is not a central volcano, are being studied in some detail.) There were several questions in mind. Had there been a compositional change in the lavas of

Eyjafjöll though time, to more alkalic, more silicic, or more iron-rich? How old is the volcano? Is there any systematic variation in the products from a single eruption, as is found for Hekla (Baldridge *et al.*, 1973)? What is the relationship of the acid rocks to the rest of the volcano; what is their extent, their composition, and their origin? A start has been made on answering all of these questions, some will require further investigation.

Figure 1. General geologic map of Iceland after K. Saemundsson, 1973 (as reprinted in Thorarinsson, 1975).

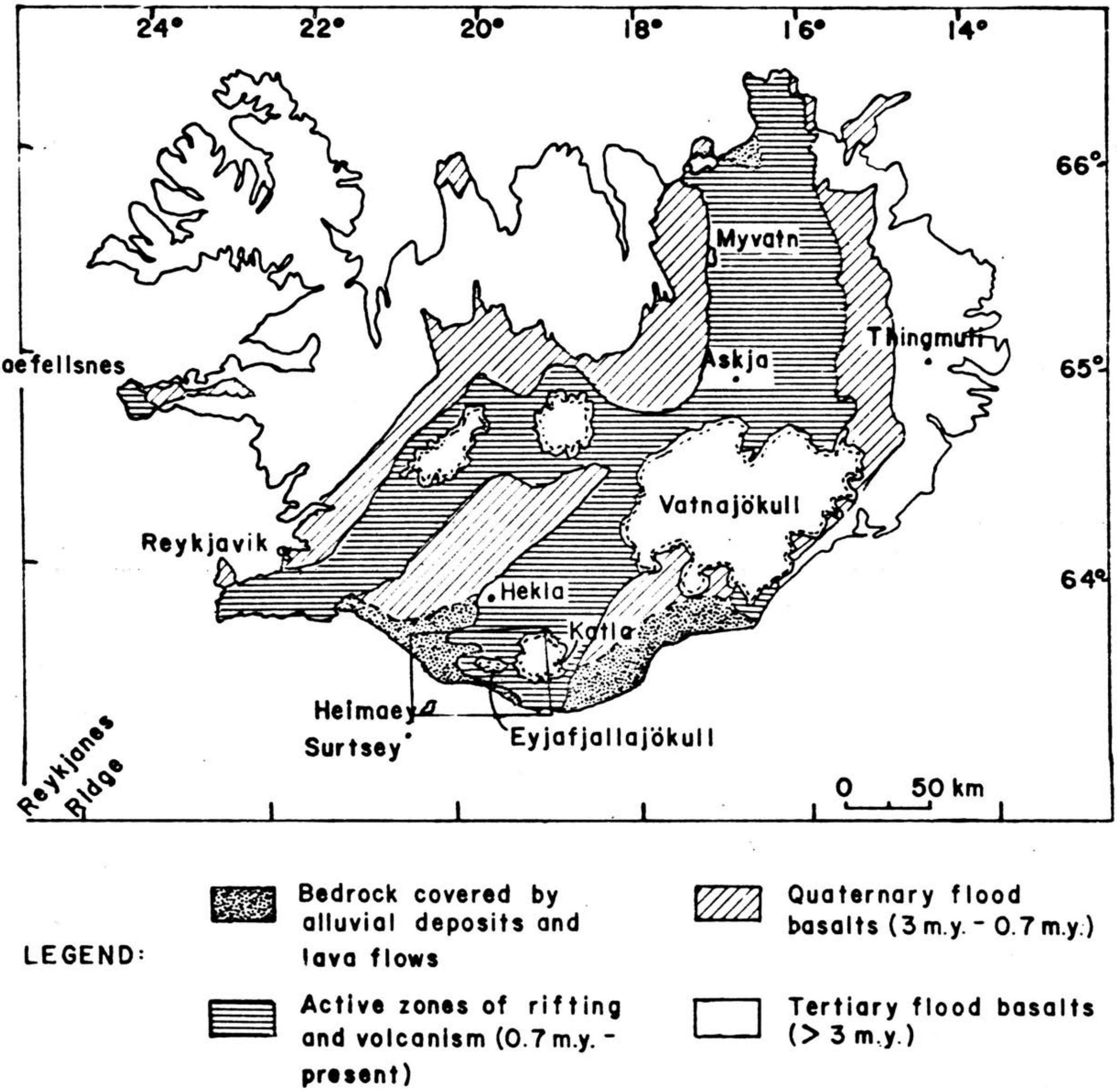

Boxed region is the area of study.

DESCRIPTION

Eyjafjöll is a composite volcano 1666 meters high, rising from the Markarfljot valley on the north and the coastal plain on the south. The central caldera is capped by the glacier Eyjafjallajökull, which in most places extends down to 850 or 900 meters elevation. The mountain is approximately 25 km in the east-west direction and 15 km north-south. On the north side of the mountain, Falljökull, a small glacier, descends from the caldera to end in a lake behind 100 m of end and side moraine. This moraine rises above and is clearly distinct from the outwash brought down from Myrdalsjökull by the Markarfljot river. There is a second small glacier to the east, which does not descend to the valley.

On the south side, the mountain ends abruptly in cliffs 200 meters high, cut by the sea before the growth of the coastal outwash plain.

Most of the eruptions on Eyjafjöll have been subglacial. The mountain is characterized by flows interlayered with tillite, pillow breccia, and irregular outcrops of "kubbaberg", a hackly-jointed rock believed formed when water covers a still-molten flow (Saemundsson, 1970; Justus, 1978). It differs from the table mountains so characteristic of subglacial eruptions in that it is a central volcano, with a central caldera and subsidiary craters on the flanks, which has erupted repeatedly over at least 10 thousand years. Table mountains form from one eruption, and do not produce differentiated rocks (Van Bemmelen and Rutten, 1955).

No attempt was made to map the volcano in detail. The sampling is believed representative of the entire mountain.

Figure 2. Map of Eyjafjöll region (after Sheet 6 of the Map of Iceland; Icelandic Geodetic Survey (1973)). Areas sampled indicated by numbered boxes.

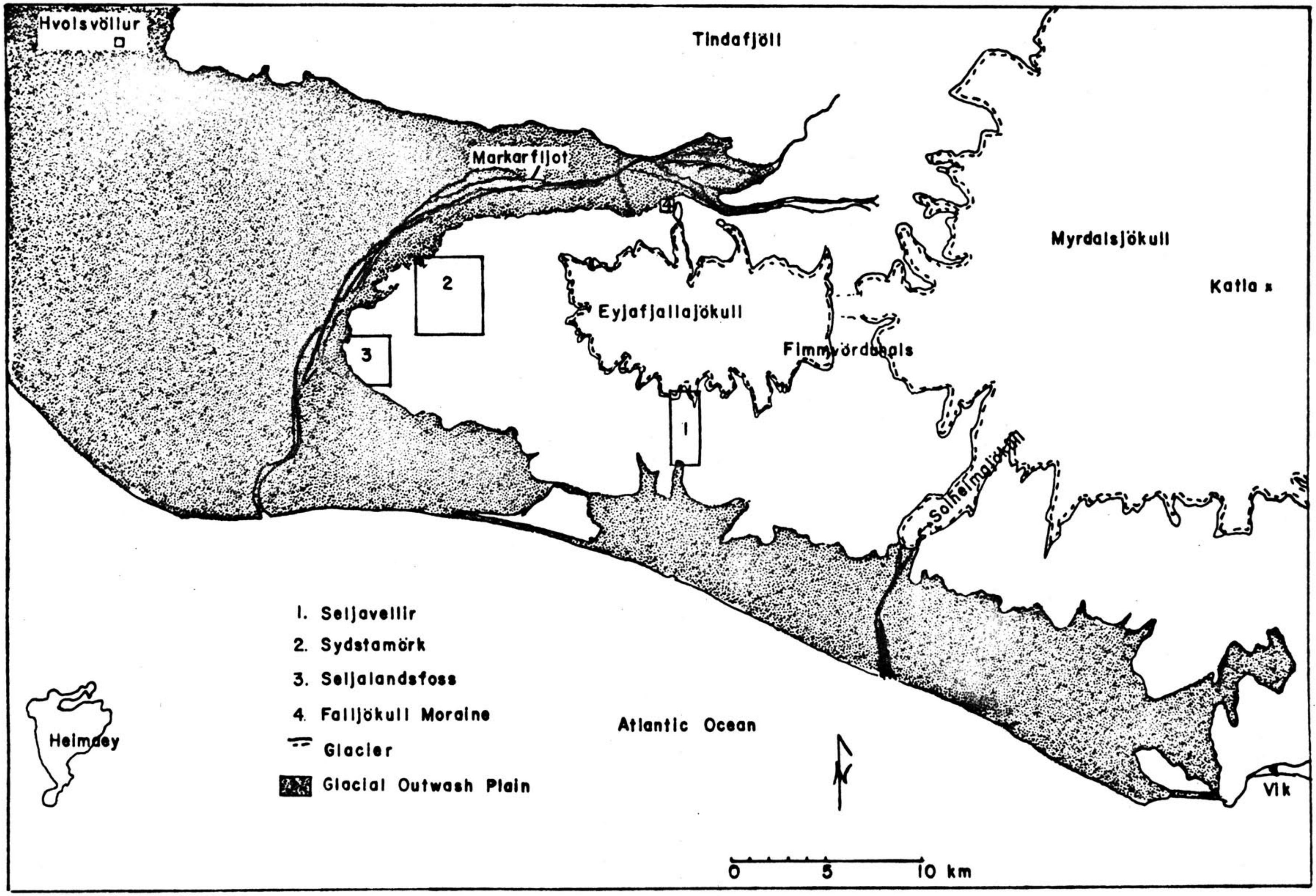
Hvolsvöllur
Tindafjöll
Markarfljot
Myrdalsjökull
Katla ×
Eyjafjallajökull
Fimmvördahals
2
3
1
4
Solheimajökull
Heimaey
Atlantic Ocean
Vik
1. Seljavellir
2. Sydstamörk
3. Seljalandsfoss
4. Falljökull Moraine
Glacier
Glacial Outwash Plain
0
5
10 km

HISTORY

Eyjafjöll has clearly been active through, and possibly before, the most recent glaciation, 10-7,000 years b.p. The oldest rocks observed are pillow breccias, hackly and irregularly jointed columns and hyaloclastics, which indicate subglacial or subaqueous origin. Glacial striae on the west flank (N5E) are consistent with the direction of movement of the last glaciation (Einarsson, 1968, p. 296). Glacial striae observed on the south side are compatible with movements of the current glacier, as well as the regional glaciation, so place no limits on the age of the flows there. Glacial striae on the northwest flank (N40W) are not consistent with the regional glaciation, but would be with an extended capping glacier larger than the present one.

The fact that the only eruption in the past 1000 years was not very voluminous suggests that the present rate of production of volcanic material could not have built up the mountain in the past 10,000 years. Based on a comparison of volume of material produced by Hekla during glacial times and in the most recent post-glacial cycle, Sigvaldason suggests that Hekla's volcanic activity has been much greater in the present cycle than in previous ones. It therefore seems possible that Eyjafjöll may have been much more active during the last glaciation than its present eruption rate would indicate, and that the large volume of subglacially erupted material might have been produced in only 3-4,000 years. The last interglacial period was 70-10,000 years b.p. (Jakobsson, pers. comm., 1977). No convincing evidence of interglacial flows was found, but the possibility should not be definitely excluded until the mountain has been mapped in detail.

All magnetic readings taken along the south side of the mountain were normal, but that is not surprising as the last reversal was .7 m.y. ago (Watkins, 1972).

Provisionally, all the tillite layers except the one at 480 meters elevation are interpreted as being the result of glacial dumping during an eruption. The tillite at 480 m. is interpreted as representing the end of the last glacial period, as the flows above it were not erupted subglacially.

The capping glacier, Eyjafjallajökull, is currently receding. In the 1800's it must have covered much more of the mountain. [Even in 1945, when the U.S. Army map (the only existing large scale map) was made, the glacier extended up to 100 meters farther down than it does now.] Movements of the present glacier complicate relative dating of flows on different parts of the mountain.

The most recent, and the only verified, historic eruption was in 1821-23. Thoroddsen (1925) also reports an eruption in 1612, but his report is based on old annals written in the north of Iceland, and Thorarinsson (1975) believes the writers confused Eyjafjallajökull with nearby Katla, as there was a Katla eruption that year.

The 1821-23 eruption was a relatively minor one, and consisted only of ash (Thoroddsen, 1925). Part of the glacier was melted at the beginning of the eruption in December, 1821, and the Markarfljot valley was flooded. The volcano continued to spew out dark ash, turning the western part of the glacier black, through December. Though the noise continued, the ash fall then stopped until late June, 1922, when it began again, dark and coarse at first, then mostly fine ash, grey and whitish in color, probably rhyolitic. It continued until June 26, 1823, when Katla began erupting. Eyjafjöll continued erupting steam for two more years (Thoroddsen, 1925).

SAMPLING

Samples were collected in 4 areas during the summer of 1975 (Fig. 2 and 3): starting at Seljavillir in the south; from Seljalandsfoss and Sydstamörk on the west and northwest flanks; and from the moraine of Falljökull on the north. Collected samples were the freshest rock obtainable and usually were approximately one kilogram; where this was not possible (i.e., pillow breccias), samples were at least 1/2 kg. Samples from the moraine were all from large blocks of rock and were also at least 1/2 kg. As the central caldera is covered by the glacier, Eyjafjallajökull, and is inaccessible for sampling, the moraine of the glacier Falljökull provides the only obtainable samples from the caldera area.

On the south side of the mountain, directly south of Falljökull and the caldera, a vertical section was sampled along the stream which flows through Seljavellir (Fig. 3a). Here the volcano has been incised deeply by the stream to expose a fairly good section. The basal portion of this section, as near as one can get to the center of the volcano, includes the oldest rocks observed.

This lowest part is composed of pillow breccias, hyaloclastites and outcrops of irregular columns and joints. The lower exposed 200 meters are cut by many dikes and sills. This is a hydrothermal area, and all of the dikes and most of the hyaloclastites are strongly altered. Quartz vug fillings are abundant, especially in the lower 150 meters exposed along the stream and on the east side of it, where the only competent rocks are altered sills. Scolecite and calcite are also found. On the west side of the stream, the lower kubbaberg is fairly fresh, and above 200 m, pillow breccias overlain by kubbaberg supplant the hyaloclastites and are above the hydrothermal area. The rest of the section is composed of variously fractured flows and minor hyaloclastites with two identifiable tillites interspersed. The section ends with a series of five glaciated flows, each 1-2 meters thick, above which there is only ground moraine from the last retreat of the present glacier. Sample 77 is a fragment of what appears to be a composite dike from the ground moraine at 750 m elevation. The outcrop was not found and probably lies under the glacier.

An attempt was made at obtaining a vertical section on the northwest flank of the mountain, southeast from Sydstamörk, but this was not possible because the stream there has not cut deeply enough into the overburden from the last glaciation (Fig. 3b). Most of the samples obtained were post-glacial, and only two, a pillow breccia and a flow, were clearly at least from an earlier time in the glaciation, if not pre-glacial. They occur below an obvious erosional surface between true "moberg", palagonatized hyaloclastite, below and a reworked moberg above. The very recent lavas which form a row of craters at the top of the shoulder (see map in Fig. 2) are clearly post-glacial. A second traverse from Sydstamörk went west to Kambagil and the Raudahraun ("red lava") cinder cone (Fig. 3b). Kambagils lava is one of the occurrences described by Kjartansson (1958). He interprets these abruptly ending lavas as the result of eruptions at the end of the last glaciation, erupted out onto the glacier. Pieces of Kambagils lava are found as disconnected outcrops sitting on sediments and till more than a mile away (see map in Fig. 3b).

Samples were also collected east and southeast of Seljalandsfoss (Fig. 3c). Here the stream Seljalandsá has not cut through the lavas, but drops 60 meters over the cliffs cut by the sea. All of this material was erupted during the last glaciation and forms a sequence of bedded ash, breccias, and discontinuous columnar flows typical of sub-glacial eruptions. Glacial striae at around 200 meters elevation clearly indicate that the lavas were covered once again by the glacier after they had cooled. The direction of striation is that of the last major glaciation (Einarsson, 1968, p. 276). The youngest flows in that area were probably erupted towards the end of that glaciation.

Figure 3. Detailed maps of areas sampled, showing sample locations and traces of cross sections given in Figure 4. After U.S. Army Corps of Engineers (1945) map of Holt area (AMS Series C762 #5717 IV). Contour intervals given in meters. a) Seljavellir; b) Sydstamörk; c) Seljalands.

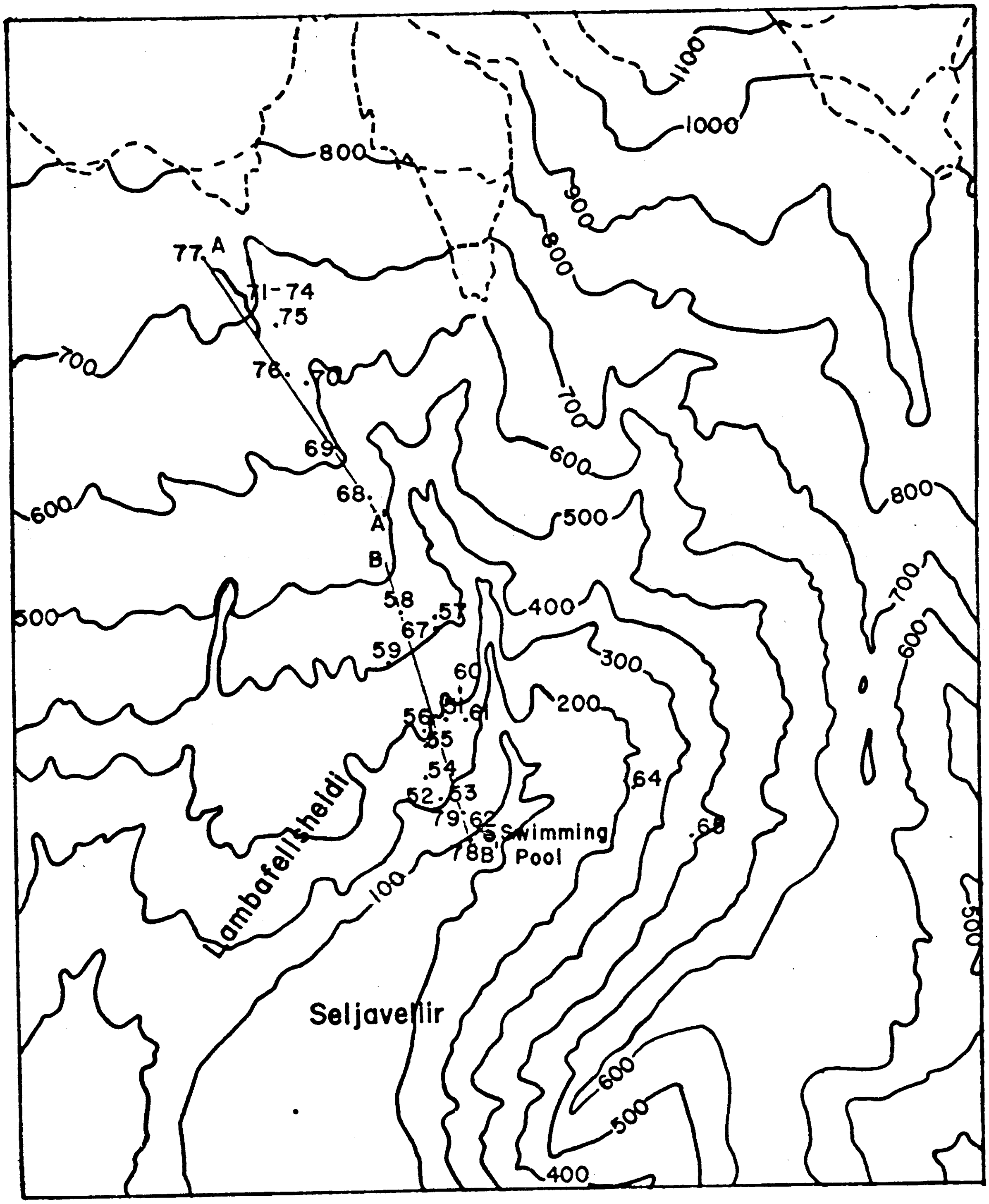
1100
1000
800
A
900
800
77
A
71-74
.75
700
76
.70
700
69
600
600
68
A'
500
B
58
.57
67
59
400
300
60
51
.61
56
.55
200
.54
52
.53
.64
79
62
Swimming Pool
.68
78
B'
100
Lambafellsheldi
800
700
600
500
Seljavellir
600
500
400

Figure 3a.

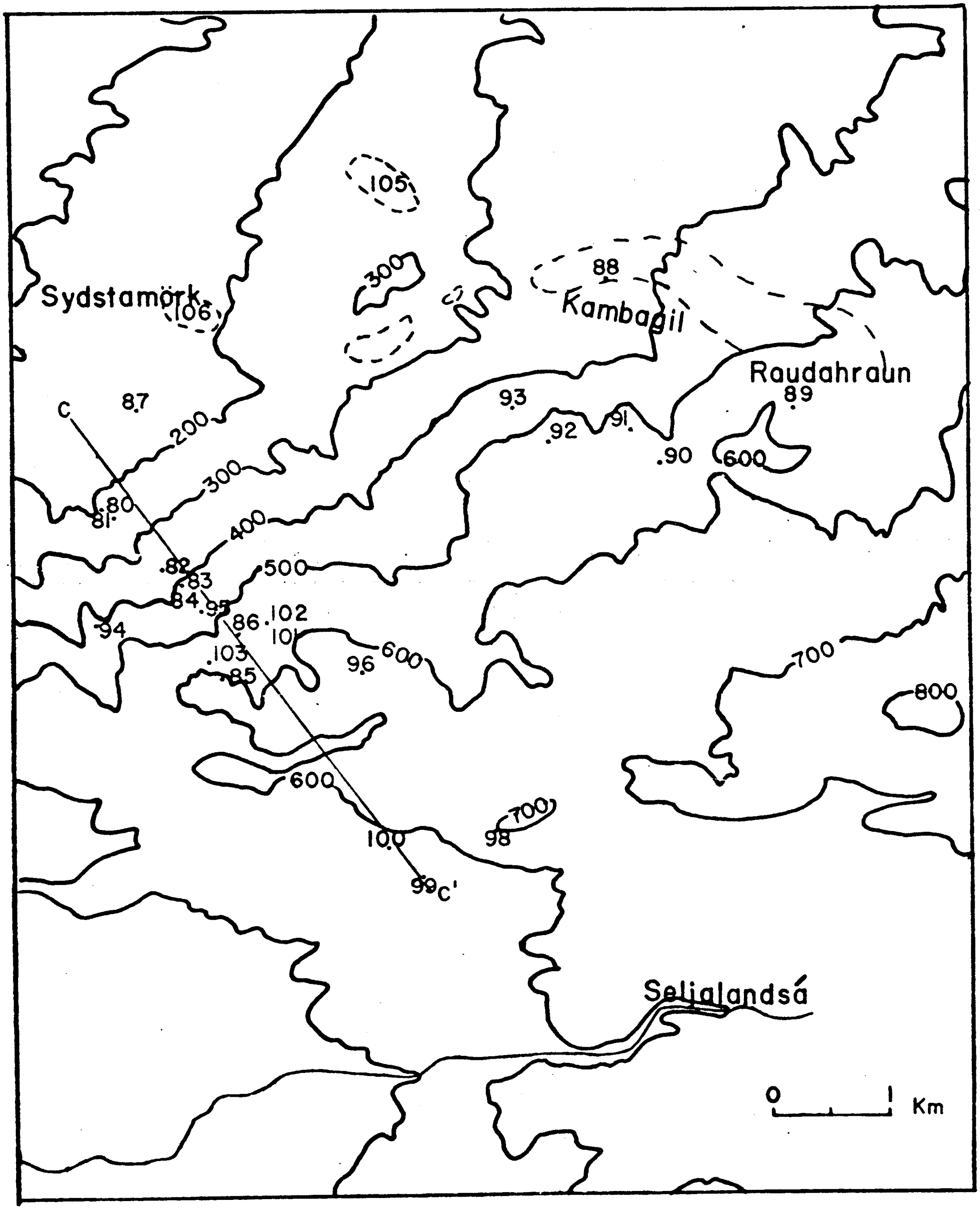
105
300
88
Sydstamörk
106
Kambagil
Raudahraun
C
87
200
93
92
91
89
90
600
300
80
81
400
82
83
500
84
95
94
86
102
101
103
85
96
600
700
800
600
700
100
98
99
C'
Seljalandsá
0
Km

Figure 3b.

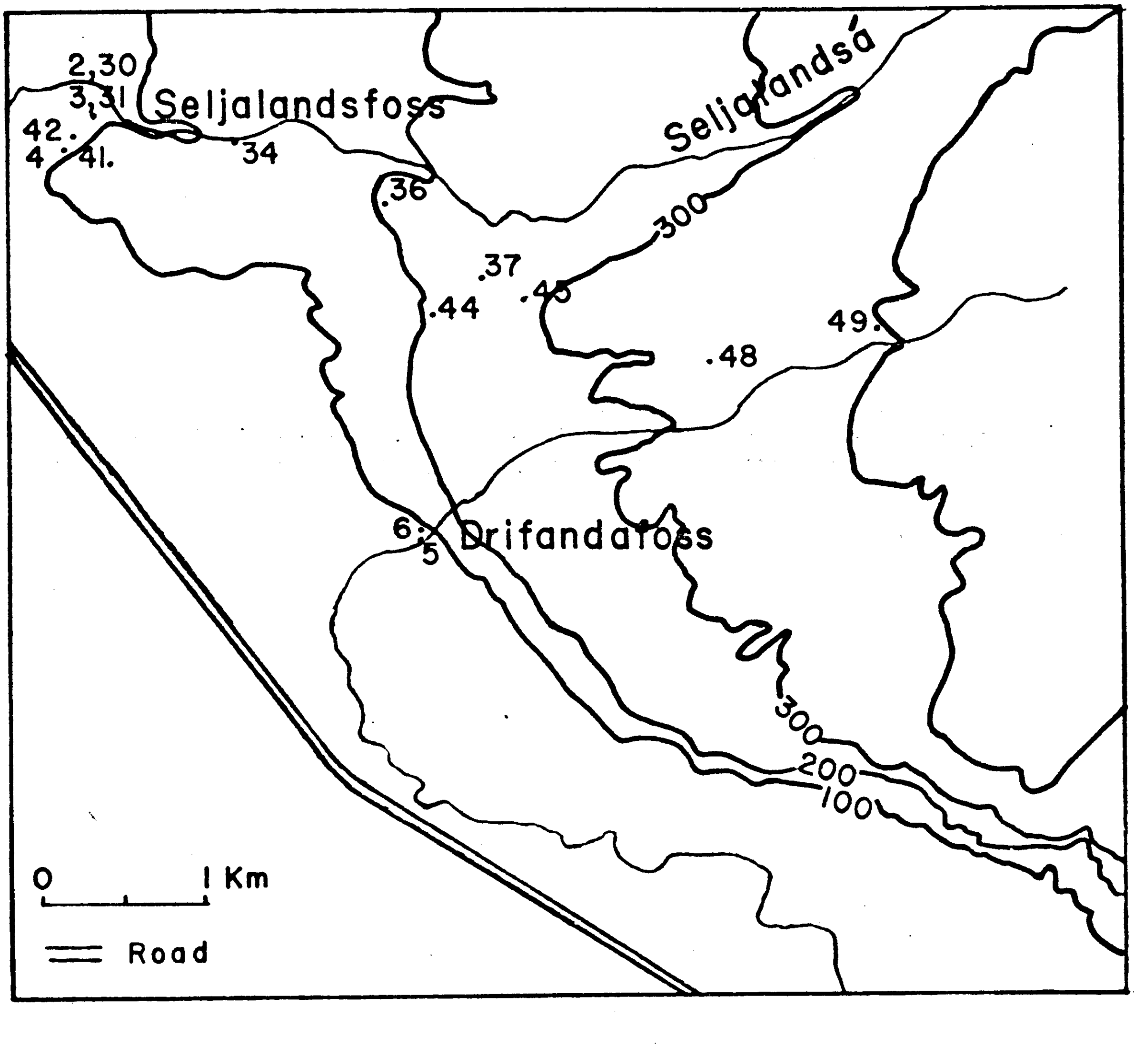
2,30
3,31
Seljalandsfoss
42.
4
41.
34
.36
Seljalandsá
300
.37
.45
.44
49.
.48
6
5
Drifandafoss
300
200
100
0
1 Km
Road

Figure 3c.

SAMPLE PREPARATION

Samples were trimmed to remove weathered edges, crushed in a jaw crusher and powdered in a tungsten carbide ball mill. They were then put through a silk screen to 200 mesh. The grinding was finished with an agate mortar and pestle as necessary. At least 200 grams of each sample were crushed, and 100 grams of that powdered to assure representative composition.

ANALYSIS

Samples were analyzed at the University of Iceland. SiO_2, Al_2O_3, Fe_2O_3, TiO_2, CaO, and K_2O were determined by X-ray fluorescence. A Philips instrument, which is neither automated nor computerized, was used. Samples were analyzed for one element at a time and a calibration curve determined using a variety of standards. Samples were prepared for XRF using the method of Rose et al. (1963). This reduced the mass absorption effects drastically as the sample was only .096 of the total glass, which contained LaO acting as the heavy absorber for most elements. Even with the lanthanum, however, calculations for the various wavelengths show that absorption effects should be significant in the measurement of SiO_2 and Al_2O_3.

Because each oxide was analyzed separately in a non-computerized set-up, the best standards were chosen for each element and a complete set of data was not obtained for each standard. This caused problems when the data were later put through a reiterative program to correct for mass absorption effects, as the program required data for all elements of each standard. Originally, all six XRF-determined oxides were corrected for mass absorption. The corrections on K_2O were seen immediately to be out of line, the error caused by the inclusion of a high-K_2O standard for the corrections, not used in the original K_2O calibration, but forced into use in the computer calibration as it was one of the few standards for which a complete set of data was available. (During the original analysis it has been the drift monitor for K_2O.) A similar problem was encountered with the Fe_2O_3 corrections, caused by the use of a standard very low in Fe_2O_3. Complete sets of data were not available for the standards which were used to determine the original Fe_2O_3 calibration. Comparison with the accepted values for the standards reveals the TiO_2 corrections also to be out of line, but it is not clear why they should be.

The uncorrected values for K_2O, TiO_2 , and Fe_2O_3 are therefore used. The mass absorption corrected values for SiO_2, Al_2O_3, and CaO are retained.

MgO and Na_2O were analyzed on a Beckman atomic absorption spectrophotometer belonging to the Nordic Volcanological Institute at the University. Samples were dissolved using HF and perchloric acid, and calibrated against Canadian Syenite-1 and a variety of in-house standards. Results are reported in Table I.

PRECISION AND ACCURACY

Seven samples were analyzed in duplicate, using the same methods of sample preparation and analysis. The results are found in Table II. In general, the agreement between duplicate analyses of the same sample was very good. Precision is believed to be no worse than the largest difference shown between replicate analyses: SiO_2 - .68%; Al_2O_3 - .41%; Fe_2O_3 - .17%; MgO - .17%; CaO - .25%; Na_2O - .48%; K_2O - .03%; TiO_2 - .06%. In most cases agreement is much better than the largest differences indicated. The large uncertainty in Na_2O applies only to Na_2O values greater than 5%, as the calibration curve had to be extrapolated for high Na_2O values. The largest Na_2O difference in the normal range of basalts was .30 wt. %.

Seven representative samples were also chosen to be analyzed by XRF at Woods Hole Oceanographic Institution. The samples were prepared using the method of Harvey _et al._, 1973. The results are shown in Table III. Again, the agreement is generally good except for samples high in SiO_2. It has been suggested (Staudigel, pers. comm.) that the problem may be caused by uneven surfaces on the glass disc caused by higher viscosity of the melt. It can be seen from Table III that the WHOI analyses of high SiO_2 rocks total over 100%. The SiO_2 values are therefore probably too high. The Iceland analyses of high SiO_2 rocks, on the other hand, have low totals, even allowing for H_2O, MnO, and P_2O_5, which were not determined. The correct silica values for the more silicic rocks probably lie somewhere between the two values.

There was a problem with the analysis of rocks with high Na_2O content at WHOI as the range of standards usually used for analyzing basalts did not extend to high enough Na_2O values to cover rhyolites or dacites. The extrapolated calibration curve produces values which are too low, as noted by Loiselle (pers. comm.) on his Belknap Mountain suite. The Na_2O values originally greater than 3.2% have, therefore, been corrected upward using Loiselle's extended calibration.

Silica and sodium in the more silicic rocks aside, the most notable difference is in TiO_2, which is consistently higher for the WHOI analyses.

Taking agreement with the Woods Hole analyses as a measure of accuracy, the analytical accuracy for most oxides in low and intermediate silica rocks is seen to be very nearly within the limits of precision as estimated above. With the exceptions noted earlier, the differences between the Iceland and WHOI analyses never exceed the limits of precision by more than .12 weight %.

TABLE I. CHEMICAL ANALYSES AND CIPW NORMS

	Seljalands											
	2	3	4	5	6	30	31	34	36	37	41	42
SiO_2	55.11	46.78	48.01	47.43	46.48	54.94	46.57	47.76	47.48	50.91	47.63	54.89
Al_2O_3	15.10	14.92	15.45	17.02	16.98	14.73	15.01	16.38	16.72	15.32	16.60	14.94
Fe_2O_3[1]	12.34	15.56	13.40	12.44	13.11	12.45	15.53	13.21	13.30	13.13	13.37	12.32
MgO	2.17	5.37	7.26	5.62	5.16	2.20	5.17	5.35	4.58	4.27	5.68	2.44
CaO	6.19	10.38	11.36	11.76	11.84	6.28	10.56	11.09	10.91	8.25	11.00	6.22
Na_2O	4.94	2.67	2.55	2.43	2.51	5.18	2.74	2.80	3.03	4.26	2.82	5.10
K_2O	1.65	.59	.48	.48	.35	1.66	.58	.53	.60	1.21	.52	1.67
TiO_2	1.70	3.60	2.65	2.62	2.90	1.69	3.60	2.89	2.95	2.92	2.90	1.71
Total[2]	99.20	99.87	101.16	99.80	99.33	99.13	99.76	100.01	99.57	100.27	100.52	99.29
MgO/MgO+FeO[3]	.19	.31	.41	.37	.34	.19	.30	.35	.31	.30	.36	.21
CIPW NORMS[3]												
Q	1.24											
Or	9.93	3.54	2.84	2.87	2.10	10.00	3.48	3.17	3.60	7.21	3.09	10.05
Ab	42.59	22.93	21.57	20.83	21.62	44.69	23.55	23.96	26.05	36.36	24.01	43.93
An	14.42	27.38	29.29	34.55	34.65	12.28	27.37	30.91	30.73	19.27	31.29	13.17
Ne												
Di	14.37	20.61	22.14	20.17	20.76	16.60	21.44	20.40	20.11	18.28	19.45	15.47
Ol		6.63	10.29	6.03	7.50	.42	7.95	7.12	8.63	9.38	9.30	.48
Hy	11.43	8.54	5.93	7.77	4.85	9.97	5.83	5.99	2.24	1.03	4.39	10.86
Il	3.29	6.94	5.03	5.04	5.61	3.27	6.95	5.55	5.69	5.59	5.54	3.31
Mt	2.73	3.43	2.91	2.75	2.91	2.77	3.43	2.90	2.95	2.88	2.93	2.73

TABLE I. (cont.)

← Seljalands / Seljavellir →

	44	45	48	49	51	52	53	54	55	56	57	58
SiO_2	47.33	47.09	46.47	46.61	51.54	48.82	49.07	48.00	51.53	51.09	50.71	52.07
Al_2O_3	16.50	17.31	17.31	17.09	15.15	15.00	15.17	15.71	15.02	15.13	15.21	14.31
Fe_2O_3[1]	12.96	13.28	13.37	13.40	13.63	14.50	14.71	14.45	13.60	13.70	13.78	15.17
MgO	5.57	4.90	4.63	4.75	3.81	4.60	4.53	4.55	3.95	3.82	4.11	3.09
CaO	11.66	11.23	11.52	11.35	7.72	9.21	9.14	9.59	7.85	7.86	8.31	7.12
Na_2O	2.55	2.74	2.68	2.78	4.05	3.44	3.56	3.35	3.92	4.22	3.75	4.16
K_2O	.48	.51	.51	.48	1.25	.97	.97	.88	1.29	1.27	1.13	1.37
TiO_2	2.71	2.86	2.77	2.91	2.71	3.38	3.44	3.41	2.77	2.76	2.62	2.61
Total[2]	99.76	99.92	99.26	99.37	99.86	99.92	100.59	99.94	99.93	99.85	99.62	99.90
MgO/MgO+FeO[3]	.36	.33	.31	.32	.27	.29	.29	.29	.28	.27	.28	.21
CIPW NORMS[3]												
Q												
Or	2.87	3.05	3.07	2.89	7.48	5.81	5.77	5.27	7.72	7.60	6.78	8.21
Ab	21.87	23.47	23.11	23.94	34.72	29.50	30.32	28.72	33.58	36.18	32.23	35.70
An	32.60	33.84	34.34	33.32	19.73	22.92	22.70	25.56	19.82	18.84	21.67	16.56
Ne												
Di	21.45	18.67	19.83	19.88	15.95	19.42	19.08	18.81	16.37	17.29	16.87	16.30
Ol	7.27	8.35	9.50	9.53	2.52	6.94	7.86	9.22	1.68	6.88	3.28	.03
Hy	5.87	4.20	1.82	1.84	11.38	5.70	4.46	2.67	12.50	4.87	11.07	14.82
Il	5.22	5.50	5.36	5.63	5.22	6.51	6.58	6.56	5.33	5.31	5.05	5.03
Mt	2.85	2.92	2.97	2.97	3.00	3.20	3.23	3.19	3.00	3.03	3.05	3.35

TABLE I. (cont.)

	Seljavellir											
	59	60	61	62	64	65	67	68	69	70	71	72
SiO_2	54.97	53.72	48.51	49.94	50.10	46.65	54.90	51.08	51.85	46.66	47.01	46.83
Al_2O_3	15.73	15.23	15.20	13.95	14.09	17.68	15.39	14.19	14.24	15.52	15.29	16.03
Fe_2O_3[1]	12.00	12.72	14.50	13.40	14.86	12.73	12.10	15.00	15.12	14.83	15.04	14.68
MgO	2.24	3.08	4.47	5.06	3.51	4.40	2.16	3.31	3.19	4.78	4.84	4.75
CaO	5.95	6.58	9.21	9.73	8.16	11.43	5.90	7.52	7.27	10.86	10.74	10.77
Na_2O	5.03	4.64	3.45	2.49	3.74	2.58	5.14	3.88	3.91	2.77	2.81	2.75
K_2O	1.72	1.57	.96	.85	1.25	.52	1.76	1.27	1.29	.59	.61	.54
TiO_2	1.82	2.17	3.47	2.79	3.24	2.36	1.73	2.65	2.78	3.30	3.40	3.22
Total[2]	99.46	99.71	99.77	98.21	98.95	98.35	99.08	98.90	99.65	99.31	99.74	99.57
MgO/MgO+FeO[3]	.20	.24	.29	.33	.24	.31	.19	.22	.22	.30	.30	.30
CIPW NORMS[3]												
Q	.50			3.35			.01	.12	1.14			
Or	10.32	9.41	5.76	5.18	7.56	3.16	10.61	7.69	7.75	3.56	3.66	3.25
Ab	43.24	39.81	29.62	21.71	32.39	22.44	44.36	33.63	33.63	23.91	24.15	23.67
An	15.51	16.31	23.50	25.11	18.39	36.11	14.00	17.98	17.79	28.83	27.73	30.31
Ne												
Di	12.30	14.12	19.01	20.36	19.36	18.43	13.49	17.08	15.95	21.79	21.92	19.97
Ol		.53	7.49		1.57	6.95				7.85	7.17	6.99
Hy	11.97	12.83	4.72	15.83	11.12	5.45	11.49	15.00	15.02	4.49	5.48	6.35
Il	3.51	4.18	6.69	5.46	6.30	4.61	3.35	5.16	5.37	6.39	6.56	6.22
Mt	2.65	2.81	3.21	3.00	3.31	2.85	2.69	3.34	3.35	3.28	3.33	3.24

TABLE I. (cont.)

← Seljavellir / Sydstamörk →

	73	74	75	76	77	78	79	80	81	82	83	84
SiO_2	46.80	47.08	47.16	52.02	63.88	52.66	52.05	45.55	46.83	46.63	53.37	50.95
Al_2O_3	15.70	16.18	16.28	14.15	14.17	15.70	15.51	13.95	15.75	16.30	14.69	14.99
Fe_2O_3[1]	14.80	14.55	14.50	14.88	7.59	12.27	12.32	16.96	14.78	13.92	13.06	13.44
MgO	4.73	4.88	4.58	3.05	.36	3.69	3.80	5.83	5.39	5.35	2.97	4.49
CaO	10.81	10.76	10.66	7.19	2.93	7.42	7.60	11.07	10.90	11.51	6.87	8.38
Na_2O	2.76	2.74	2.72	3.87	5.18	4.46	4.48	2.59	2.75	2.62	4.40	3.73
K_2O	.58	.57	.57	1.35	2.94	1.50	1.49	.51	.63	.56	1.52	1.12
TiO_2	3.23	3.17	3.24	2.52	.63	2.39	2.40	3.63	3.15	2.82	2.41	2.68
Total[2]	99.41	99.93	99.71	99.03	97.68	100.09	99.65	100.09	100.18	99.71	99.29	99.78
MgO/MgO+FeO[3]	.29	.30	.29	.21	.06	.28	.29	.31	.32	.33	.23	.30
CIPW NORMS[3]												
Q				1.62	13.82						.96	
Or	3.49	3.41	3.42	8.16	17.90	8.95	8.93	3.06	3.76	3.36	9.15	6.71
Ab	23.79	23.49	23.37	33.50	45.17	38.11	38.45	22.22	23.52	22.50	37.92	31.99
An	29.28	30.57	31.00	17.65	6.94	18.57	18.06	25.27	29.09	31.52	16.14	21.14
Ne												
Di	21.09	19.53	18.88	15.94	7.07	15.52	16.82	25.22	21.18	21.86	15.66	17.46
Ol	7.26	7.03	4.89			5.19	7.93	13.03	10.62	10.67		2.95
Hy	5.56	6.67	8.98	14.93	6.17	6.39	2.47	.48	2.53	1.57	12.62	11.62
Il	6.25	6.10	6.25	4.89	1.23	4.58	4.62	6.99	6.05	5.44	4.66	5.16
Mt	3.28	3.20	3.21	3.31	1.70	2.69	2.72	3.73	3.25	3.08	2.89	2.97

TABLE I. (cont.)

	Sydstamörk											
	85	86	87	88	89	90	91	92	93	94	95	96
SiO_2	51.80	51.79	52.13	52.18	51.87	51.67	51.78	48.11	56.47	51.79	50.95	52.12
Al_2O_3	15.21	15.36	15.57	15.31	15.89	15.43	15.43	14.45	14.90	14.91	14.94	14.91
Fe_2O_3[1]	13.27	13.04	13.04	12.89	13.09	13.23	13.23	14.80	11.66	13.04	13.52	13.25
MgO	3.97	4.11	3.83	3.81	3.63	3.43	3.50	8.27	2.04	4.21	4.51	4.10
CaO	7.79	7.83	8.08	8.08	7.69	7.51	7.40	10.34	5.58	7.95	8.38	7.83
Na_2O	3.78	3.79	3.77	3.64	3.25	4.89	4.88	2.78	5.16	3.93	3.94	3.88
K_2O	1.14	1.18	1.18	1.21	.88	1.34	1.39	.59	1.78	1.19	1.14	1.14
TiO_2	2.60	2.60	2.41	2.34	2.35	2.84	2.72	3.29	1.65	2.60	2.66	2.55
Total[2]	99.56	99.70	100.01	99.46	98.65	100.34	100.33	102.63	99.24	99.62	100.04	99.78
MgO/MgO+FeO[3]	.28	.29	.28	.28	.27	.25	.26	.42	.19	.30	.30	.29
CPIW NORMS[3]												
Q	.84	.45	.77	1.59	4.54				2.47			.59
Or	6.84	7.07	7.05	7.27	5.33	7.98	8.28	3.44	10.71	7.14	6.81	6.83
Ab	32.49	32.53	32.26	31.31	28.20	39.36	39.43	23.20	44.44	33.76	33.71	33.28
An	21.51	21.72	22.32	22.23	26.83	16.32	16.22	24.87	12.45	19.82	19.93	20.17
Ne						1.27	1.19					
Di	14.82	14.73	15.21	15.48	10.29	17.78	17.41	21.00	13.39	16.82	18.38	16.01
Ol						8.95	9.37	14.14		.80	6.22	
Hy	15.55	15.61	14.89	14.76	17.32			4.01	10.77	13.76	6.86	15.28
Il	5.02	5.01	4.63	4.52	4.58	5.44	5.21	6.16	3.19	5.01	5.11	4.91
Mt	2.93	2.88	2.87	2.84	2.91	2.90	2.89	3.18	2.58	2.89	2.98	2.93

TABLE I. (cont.)

								← Sydstamörk / Falljökull Moraine →				
	98	99	100	101	102	103	104	105	106	107	108	109
SiO_2	52.32	49.17	49.54	51.83	51.92	52.43	52.37	52.47	52.63	66.91	55.01	54.93
Al_2O_3	15.22	14.77	14.56	15.00	15.09	15.31	14.85	15.26	15.48	14.22	15.80	15.16
Fe_2O_3[1]	13.07	14.87	14.75	13.10	13.02	12.97	13.21	12.77	12.82	5.02	11.25	12.03
MgO	4.00	4.96	4.89	4.32	4.25	3.87	3.98	3.80	3.81	.19	2.55	2.64
CaO	7.64	8.88	8.93	8.01	7.87	7.62	7.73	7.90	7.85	1.82	6.04	6.31
Na_2O	3.85	3.46	3.42	3.59	3.47	3.79	3.70	3.52	3.25	5.80	4.94	4.24
K_2O	1.14	.93	.93	1.15	1.13	1.19	1.21	1.20	1.16	3.33	1.87	1.70
TiO_2	2.57	3.31	3.26	2.58	2.57	2.47	2.52	2.26	2.34	.43	1.94	2.03
Total[2]	99.81	100.35	100.28	99.58	99.32	99.65	99.57	99.18	99.34	97.72	99.40	99.04
MgO/MgO+FeO[3]	.29	.30	.30	.30	.30	.28	.28	.28	.28	.05	.23	.22
CIPW NORMS[3]												
Q	1.23			1.22	2.21	1.63	1.83	2.76	4.32	15.38	.43	3.92
Or	6.82	5.55	5.55	6.90	6.80	7.14	7.26	7.23	6.98	20.23	11.23	10.25
Ab	33.01	29.55	29.23	30.85	29.90	32.54	31.81	30.36	27.99	50.44	42.46	36.61
An	21.15	22.23	21.84	21.75	22.67	21.56	20.66	22.73	24.66	3.01	15.66	17.67
Ne												
Di	14.38	18.46	19.01	15.47	14.21	14.02	15.27	14.39	12.51	5.52	12.46	12.05
Ol		6.71	4.53									
Hy	15.58	7.90	10.35	15.93	16.36	15.48	15.39	15.31	16.19	3.46	11.53	12.91
Il	4.95	6.34	6.25	4.98	4.97	4.76	4.86	4.38	4.52	.84	3.74	3.93
Mt	2.88	3.26	3.24	2.90	2.88	2.87	2.92	2.84	2.83	1.12	2.49	2.66

TABLE I. (cont.)

Falljökull Moraine

	110	111	112	113
SiO_2	66.88	64.92	66.65	54.63
Al_2O_3	13.78	15.81	13.99	15.52
Fe_2O_3[1]	5.69	5.09	5.80	11.94
MgO	.20	.20	.03	2.57
CaO	1.77	1.63	1.67	6.18
Na_2O	5.98	6.23	6.10	4.44
K_2O	3.33	3.77	3.34	1.73
TiO_2	.39	.43	.33	1.95
Total[2]	98.02	98.08	97.91	98.96
MgO/MgO+FeO[3]	.04	.05	.01	.22
CIPW NORMS[3]				
Q	14.29	8.90	13.57	2.55
Or	20.18	22.81	20.26	10.44
Ab	51.88	53.99	52.98	38.36
An	.95	4.14	.95	17.67
Ne				
Di	7.10	3.65	6.72	11.52
Ol				
Hy	3.58	4.54	3.58	13.03
Il	.76	.84	.64	3.78
Mt	1.26	1.13	1.30	2.65

[1] Total Fe as Fe_2O_3.

[2] Totals include total Fe as Fe_2O_3. P_2O_5, MnO, and H_2O were not determined.

[3] In the calculation of CIPW norms, Fe_2O_3 was set at .15 of the determined Fe_2O_3. The rest was re-calculated to FeO. The MgO/MgO+Fe ratio uses the calculated FeO.

TABLE II. DUPLICATE ANALYSES - ICELAND

	37	37	62	62	71	71	77	77
SiO_2	50.69	50.91	49.92	49.94	46.90	47.01	63.89	63.88
Al_2O_3	15.48	15.32	14.30	13.95	15.70	15.29	14.11	14.17
Fe_2O_3[1]	13.20	13.13	13.23	13.40	15.11	15.04	7.55	7.59
MgO	4.37	4.27	4.93	5.06	4.97	4.84	.37	.36
CaO	8.15	8.25	9.64	9.73	10.68	10.74	2.93	2.93
Na_2O	4.06	4.26	2.45	2.49	2.76	2.81	5.36	5.18
K_2O	1.21	1.21	.83	.85	.61	.61	2.91	2.94
TiO_2	2.93	2.92	2.73	2.79	3.40	3.40	.64	.63
Total	100.09	100.27	98.03	98.21	100.13	99.74	97.76	97.68

	88	88	92	92	107	107
SiO	52.60	52.18	47.43	48.11	67.25	66.91
Al_2O_3	15.37	15.31	14.41	14.45	13.94	14.22
Fe_2O_3[1]	12.90	12.89	14.85	14.80	4.97	5.02
MgO	3.78	3.81	8.11	8.27	.17	.19
CaO	7.99	8.08	10.59	10.34	1.83	1.82
Na_2O	3.94	3.64	2.67	2.78	6.28	5.80
K_2O	1.20	1.21	.60	.59	3.32	3.33
TiO_2	2.36	2.34	3.27	3.29	.43	.43
Total	100.14	99.46	101.93	102.63	98.19	97.72

[1] Total FeO as Fe_2O_3.

TABLE III. DUPLICATE ANALYSES - WOODS HOLE

	2	WHOI	37	WHOI	73	WHOI	82	WHOI
SiO_2	55.11	56.12	50.91	50.33	46.80	47.25	46.63	47.20
Al_2O_3	15.10	15.33	15.32	15.82	15.70	15.73	16.30	16.43
FeO[1]	11.10	10.95	11.81	11.90	13.32	13.61	12.53	12.75
MgO	2.17	2.33	4.27	4.23	4.73	4.79	5.35	5.39
CaO	6.19	6.13	8.25	8.19	10.81	11.18	11.51	11.75
Na_2O	4.94	4.75[2]	4.26	4.17[2]	2.76	2.48	2.62	2.55
K_2O	1.65	1.65	1.21	1.18	.58	.54	.56	.54
TiO_2	1.70	1.78	2.92	3.04	3.23	3.43	2.82	2.99
P_2O_5		.57		.70		.32		.25
Total	97.96	99.61	98.95	99.56	97.93	99.33	98.32	99.85

	93	WHOI	96	WHOI	110	WHOI
SiO_2	56.47	58.85	52.12	51.96	66.88	70.35
Al_2O_3	14.90	14.93	14.91	14.99	13.78	13.95
FeO[1]	10.49	10.45	11.92	11.90	5.12	4.99
MgO	2.04	2.10	4.10	3.99	.20	.27
CaO	5.58	5.57	7.83	7.90	1.77	1.44
Na_2O	5.16	5.04[2]	3.88	3.35[2]	5.98	6.49[2]
K_2O	1.78	1.77	1.14	1.12	3.33	3.35
TiO_2	1.65	1.71	2.55	2.68	.39	.44
P_2O_5		.62		.78		.05
Total	98.07	101.04	98.45	98.67	97.45	101.33

[1] Total Fe as FeO. Analyses done in Iceland as Fe_2O_3 re-calculated for comparison.

[2] See text for explanation.

CHEMICAL GROUPING

As a first step in interpreting the data, samples were subdivided according to locality. Seljavellir and the moraine samples were taken together as the two lie directly south and north of the caldera and are closest to it. (As it turned out the groupings did not overlap for the two areas.) Seljalands and Sydstamörk on the west and northwest flanks were taken separately.

The samples within a locality were then grouped. The compositional range within a group (lowest to highest), was 1.10% for SiO_2, .80% for Al_2O_3, .80% for Fe_2O_3, .50% for MgO and CaO, .40% for Na_2O, .10% for K_2O, and .30% for TiO_2. Analyses were grouped first by SiO_2, then checked to see if they met the range limits for K_2O, TiO_2, Fe_2O_3, and MgO, in that order, followed by Al_2O_3, CaO, and Na_2O. The first five oxides define the group, and once extraneous samples are eliminated on the basis of these oxides, the other oxides usually fit the group. The results are shown in Table IV. The two samples which fit a group well except for Al_2O_3 and Na_2O were not included in calculations of the group averages, but are listed in parentheses with the group.

Limits were set as narrowly as possible, still including within a group all the samples which by field and petrographic evidence belonged to it. In some cases, this meant eliminating samples from a group of very near composition because of unusual TiO_2 or Fe_2O_3 values. It was believed better to make the groups more restrictive than to expand the range of an element to accomodate one particular sample or another which did not quite fit its field-indicated group.

Groups are listed in Table IV in order of eruption for each area. Location and descriptions of samples are given in Table V. For Seljalands, determining the order of eruption was relatively easy since the stratigraphy is fairly clear, except for the relationship between the lower units at Drifandafoss and those at Seljalandsfoss. It seems likely that the Drifandafoss flows came first, as that area is somewhat closer to the center of the volcano. In any case, flows 36 and 45-49 are more recent than either the lower Seljalands or Drifandafoss.

For the Sydstamörk suite, the stratigraphy is not so simple because erosion (by sea or stream) has not exposed a section. Samples 81 and 82 are very early glacial or preglacial, as is 92. The flow represented by samples 99 and 100 may also have been glaciated. It is not clear where the dike (80) belongs; as it cuts sediments and conglomerates which are below 81 in elevation, but of unknown age. Many of the sediments at that elevation are recent, and it is not possible to tell the relative age of these. No other rocks like 80 were found anywhere on the mountain. The dike 83 cuts the kubbaberg 84 and may have been intruded any time after the formation of 84 and 95. As previously mentioned, Kambagils lava (87, 88, 105, 106) is late glacial. Raudahraun, 89, forms a large cinder cone above Kambagils lava and is obviously post-glacial, though not of the same composition as the large group of post-glacial lavas and cinders grouped as "recent." These latter rocks show remarkably constant composition. They were erupted from a series of craters along a fissure on the northwest flank (S. Jakobsson, pers. comm., 1975). It is not clear where in time sample 93 belongs. It is from a shoulder of black cinders, obviously late or post-glacial, but in elevation below glaciated 92. The composition closely resembles that obtained by N. Oskarsson for SAL38, collected by S. Thorarinsson as a sample of the 1821-23 eruption. Sample 93 might also be from that eruption.

The Seljavellir stratigraphy is also fairly clear, until one reaches the last outcrops beneath the ground moraine above 700 meters elevation. The flow represented by samples 58, 68, 69, and 76 is listed as stratigraphically above 70-74 on the basis of outctop 74 overlying outcrop 70. Samples 70-74 are from a series of thin, even flows and have been thoroughly glaciated. Samples 58, 68, and 69 directly overlie a severely glaciated tillite. The top of the flow (58) also appears glaciated. As previously mentioned, the presence of a glacier which is currently receding not far from these outcrops creates some doubt as to the time scale of these glaciations. The flow represented by 58, 68, 69, and 76 was erupted onto wet ground, but not sub-glacially. Both the series of flows 70-74 and flow 58, 68, 69, 76, clearly represent post-glacial eruptions, which have since been glaciated themselves.

The samples from Falljökull moraine obviously could not be listed by stratigraphy (which is completely unknown) and are listed in order of increasing SiO_2 content.

TABLE IV. GROUP AVERAGE CHEMICAL ANALYSES AND CIPW NORMS

Seljalands - Drifandafoss

	5,44	6	2,30,42	3,31	4	34,41	36	37	45,48,49
SiO_2	47.38	46.48	54.98	46.68	48.01	47.70	47.48	50.91	46.72
Al_2O_3	16.76	16.98	14.92	14.97	15.45	16.49	16.72	15.32	17.24
Fe_2O_3[1]	12.70	13.11	12.37	15.55	13.40	13.29	13.30	13.13	13.35
MgO	5.60	5.16	2.27	5.27	7.26	5.52	4.58	4.27	4.76
CaO	11.71	11.84	6.23	10.47	11.36	11.05	10.91	8.25	11.37
Na_2O	2.49	2.51	5.07	2.71	2.55	2.81	3.03	4.26	2.73
K_2O	.48	.35	1.66	.59	.48	.53	.60	1.21	.50
TiO_2	2.67	2.90	1.70	3.60	2.65	2.90	2.95	2.92	2.85
Total	99.79	99.33	99.20	99.84	101.16	100.29	99.57	100.27	99.52
Total Fe as FeO	11.43	11.80	11.13	13.99	12.06	11.96	11.97	11.81	12.01
CIPW NORMS[2]									
Q			.33						
Or	2.87	2.10	9.99	3.54	2.84	3.16	3.60	7.21	3.00
Ab	21.34	21.62	43.71	23.28	21.57	23.98	26.05	36.36	23.48
An	33.57	34.65	13.30	27.35	29.29	31.08	30.73	19.27	33.86
Ne									
Di	20.81	20.76	15.47	21.04	22.14	19.95	20.11	18.28	19.45
Ol	6.65	7.50		7.39	10.29	8.26	8.63	9.38	9.09
Hy	6.81	4.85	11.15	7.03	5.93	5.10	2.24	1.03	2.66
Il	5.14	5.61	3.29	6.94	5.03	5.56	5.69	5.59	5.50
Mt	2.81	2.91	2.75	3.43	2.91	2.91	2.95	2.88	2.95

TABLE IV. (cont.)

Sydstamörk

	80	81	82	92	99,100	84,95	83	90,91	87,88,105 (106)	89
SiO_2	45.55	46.83	46.63	48.11	49.36	50.95	53.37	51.73	52.26	51.87
Al_2O_3	13.95	15.75	16.30	14.45	14.67	14.97	14.69	15.43	15.38	15.89
Fe_2O_3[1]	16.96	14.78	13.92	14.80	14.81	13.48	13.06	13.23	12.90	13.09
MgO	5.83	5.39	5.35	8.27	4.93	4.50	2.97	3.47	3.81	3.63
CaO	11.07	10.90	11.51	10.34	8.91	8.38	6.87	7.46	8.02	7.69
Na_2O	2.59	2.75	2.62	2.78	3.44	3.84	4.40	4.89	3.64	3.25
K_2O	.51	.63	.56	.59	.93	1.13	1.52	1.37	1.20	.88
TiO_2	3.63	3.15	2.82	3.29	3.29	2.67	2.41	2.78	2.34	2.35
Total	100.09	100.18	99.71	102.63	100.34	99.92	99.29	100.36	99.55	98.65
Total Fe as FeO	15.26	13.30	12.53	13.32	13.33	12.13	11.75	11.90	11.61	11.78
CIPW NORMS[2]										
Q							.96		1.72	4.54
Or	3.06	3.76	3.36	3.44	5.55	6.76	9.15	8.16	7.20	5.33
Ab	22.22	23.52	22.50	23.20	29.38	32.90	37.92	39.32	31.28	28.20
An	25.27	29.09	31.52	24.87	22.04	20.53	16.14	16.23	22.43	26.83
Ne								1.29		
Di	25.22	21.18	21.86	21.00	18.73	17.93	15.66	17.64	15.02	10.29
Ol	13.03	10.62	10.67	14.14	5.65	4.67		9.15		
Hy	.48	2.53	1.57	4.01	9.09	9.12	12.62		14.98	17.32
Il	6.99	6.05	5.44	6.16	6.31	5.13	4.66	5.32	4.51	4.58
Mt	3.73	3.25	3.08	3.18	3.25	2.96	2.89	2.89	2.86	2.91

TABLE IV. (cont.)

	Sydstamörk			Falljökull Moraine			
	85,86,94,96,98 101,103,104,(102)	93	SAL38[3]	109,113	108	111	107,110,112
SiO_2	52.06	56.47	56.80	54.78	55.01	64.92	66.81
Al_2O_3	15.10	14.90	14.65	15.34	15.80	15.81	14.00
Fe_2O_3[1]	13.12	11.66	10.74[4]	11.99	11.25	5.09	5.50
MgO	4.07	2.04	2.06	2.61	2.55	.20	.14
CaO	7.80	5.58	5.34	6.25	6.04	1.63	1.75
Na_2O	3.79	5.16	4.43	4.34	4.94	6.23	5.96
K_2O	1.17	1.78	1.47	1.72	1.87	3.77	3.33
TiO_2	2.56	1.65	1.86	1.99	1.94	.43	.38
Total	99.67	99.24	97.35	99.02	99.40	98.08	97.87
Total Fe as FeO	11.81	10.49	9.66[4]	10.79	10.12	4.58	4.95
CIPW NORMS[2]							
Q	.93	2.47	8.66	3.20	.43	8.90	14.42
Or	7.02	10.71	9.01	10.37	11.23	22.81	20.20
Ab	32.54	44.44	38.87	37.47	42.46	53.99	51.77
An	21.04	12.45	16.33	17.65	15.66	4.14	1.65
Ne							
Di	15.19	13.39	9.45	11.82	12.46	3.65	6.42
Ol							
Hy	15.45	10.77	11.60	12.97	11.53	4.54	3.56
Il	4.93	3.19	3.66	3.86	3.74	.84	.74
Mt	2.90	2.58	2.42	2.66	2.49	1.13	1.24

TABLE IV. (cont.)

Seljavellir

	78,79	62	52,53 54,61	51,55 56	60	59,67	57	75	70–73 (74)	58,76 68,69	77
SiO_2	52.36	49.94	48.60	51.39	53.72	54.94	50.71	47.16	46.83	51.76	63.88
Al_2O_3	15.61	13.95	15.27	15.10	15.23	15.56	15.21	16.28	15.64	14.22	14.17
Fe_2O_3[1]	12.30	13.40	14.54	13.64	12.72	12.05	13.78	14.50	14.84	15.04	7.59
MgO	3.75	5.06	4.54	3.86	3.08	2.20	4.11	4.58	4.78	3.16	.36
CaO	7.51	9.73	9.29	7.81	6.58	5.93	8.31	10.66	10.80	7.28	2.93
Na_2O	4.47	2.49	3.45	4.06	4.64	5.09	3.75	2.72	2.77	3.96	5.18
K_2O	1.50	.85	.95	1.27	1.57	1.74	1.13	.57	.58	1.32	2.94
TiO_2	2.40	2.79	3.43	2.75	2.17	1.78	2.62	3.24	3.29	2.64	.63
Total	99.90	98.21	100.07	99.88	99.71	99.29	99.62	99.71	99.53	99.38	97.68
Total Fe as FeO	11.07	12.06	13.08	12.27	11.45	10.84	12.40	13.05	13.35	13.53	6.83
CIPW NORMS[2]											
Q		3.35				.23				.70	13.82
Or	8.96	5.18	5.68	7.60	9.41	10.46	6.78	3.42	3.49	7.95	17.90
Ab	38.26	21.71	29.54	34.80	39.81	43.83	32.23	23.37	23.69	34.16	45.17
An	18.31	25.11	23.65	19.48	16.31	14.73	21.67	31.00	29.13	17.46	6.94
Ne											
Di	16.16	20.36	19.10	16.53	14.12	12.93	16.87	18.88	21.11	16.36	7.07
Ol	6.63		7.94	3.61	.53		3.28	4.89	7.04		
Hy	4.36	15.83	4.30	9.68	12.83	11.71	11.07	8.98	5.90	14.92	6.17
Il	4.61	5.46	6.59	5.29	4.18	3.44	5.05	6.25	6.36	5.11	1.23
Mt	2.71	3.00	3.20	3.01	2.81	2.67	3.05	3.21	3.28	3.34	1.70

TABLE IV. (cont.)

[1] Total FeO as Fe_2O_3.

[2] In the calculation of CIPW norms Fe_2O_3 was set at .15 the determined Fe_2O_3.

[3] SAL38 collected by S. Thorarinsson, analyzed by N. Oskarsson.

[4] Total Fe as Fe_2O_3 and FeO recalculated from the reported value $Fe_2O_3 = 2.96$, FeO = 7.00.

TABLE V. SAMPLE DESCRIPTION AND APPPROXIMATE ELEVATION

Seljalands

Sample Numbers	Approximate Elevation (m)	Description
Drifandafoss		
5	40	Pillow breccia under tuff. Lowermost visible layer at Drifandafoss.
6	50	Lower basalt flow above tuff.
44	220	Glaciated flow.
Seljalandsfoss		
2,30,42	40	Vesicular cinder blocks from bedded ash at Seljalandsfoss.
31	40	Fragment of breccia in ash.
3	45	Breccia in place.
4	50	Extremely prophyritic columns between ash and breccia.
34,41	120-130	Along Seljalandsá: 34 - flow, 6-8 m thick; 41 - just below glaciated outcrop.
36	200-240	Massive flow.
37	250-265	Flow laminated, 2-4 cm, flat breaking on lamination, perhaps intrusion?
45-49	280-360	(Late glacial?) flows. Plagioclase phenocrysts to 3 mm long.

TABLE V. (cont.)

Sydstamörk, up Ljosa

Sample Numbers		Approximate Elevation (m)	Description
80		220	Dike ∿3 m thick. Cuts breccia and conglomerate Slightly porphyritic.
81		250	Pillow breccia with few whole pillows. Very plagioclase prophyritic, some olivine.
Conglomerate-tillite			
Ash beds			
82		365-370	Flow ∿2 m thick.
Moberg ∿3 m		390	
Erosional surface			
Reworked mob. ∿4-6 m			
83		400	'Dike", linear feature but possibly flow or kubbaberg.
84-95		410-500	Kubbaberg.
94	"recent"	445	Outcrop at edge of Hrafngil in till. Possibly dike.
85		580	Top of recent lava.
86		550	Kubbaberg.
96		630	Massive flow. Some lineation of vesicles.
98		660	Vesicular flow banded lava from cinder crater.
101		585	Massive flow, 3 m thick, at top of Ljósá channel.
102			Cinder on which flow 101 rests.
103		590-600	Massive block of flow, west of but near 85. Smooth face.
104			Piece of 103 from slope below.

TABLE V. (cont.)

Sample Numbers		Approximate Elevation (m)	Description
Sydstamörk, up Ljósá			
99,100		600	Smooth rounded outcrops. No striae, but look glaciated. More relief than 70-75. 100 has cleavage like 37, 91, 56.
Sydstamörk, toward Kambagil			
87	Kambigils lava	130	Flow ∿2 m thick. Below sediments of sand and gravel. Follows topography.
88		350	Kambagil lava at Kambagil.
105		230-280	Flow on top of sediments on side of hill. Conformable with sediments.
106		165	Flow in small valley between hills of sediment.
93		400	Shoulder covered with black scoria and bombs to 1/2 m. Does not continue beyond ravine.
92		495	Very porphyritic, olivine and plagiocalse rich. Glaciated top with striae and grooves. 10-15 m thick flow whose bottom rests on stratified sediments.
90-91		500-510	Kiln-shaped outcrop and flat cleavage blocks. Rests on thin layer of ash.
89		565	Raudahraun crater. Cinder cone, whole crater is scoria and bombs.

TABLE V. (cont.)

Seljavellir

Sample Numbers	Approximate Elevation (m)	Description
78,79	80-170	Kubbaberg and roseate columns in pillow breccia.
62	90-100	Dike cutting pillow breccia in hydrothermal area.
52,53,54,61	200-280	Pillow breccia (52). Parts of flows (53-54) with hyaloclastites and sediments between.
51,55,56	280-300	Radiating columns, pillow breccia.
60	300-320	Probably part of flow; left as promontory.
Slope of sediment		
59,67	400-430	Fine grained black kubbaberg.
57	∿430	Flow ∿2 m thick.
Tillite-glaciated		
58,76,68,69	490-645	Flow. Oxidized base. Flowed down hill and overlies tillite.
75	∿660-670	Flow, glaciated, 2-3 m thick, also flowed downhill.
70-74	640,680-740	71-74: series of plagioclase porphyritic flows. Post-glacial, 1-2 m thick. 70 - irregular outcrop overlies ash and cinder layer, irregular base, no pillow breccia underlying.
77	750	Fragment, believed of composite dike in ground moraine.

Figure 4a. Cross-section near Seljavellir.

Figure 4b. Cross-section near Sydstamörk.

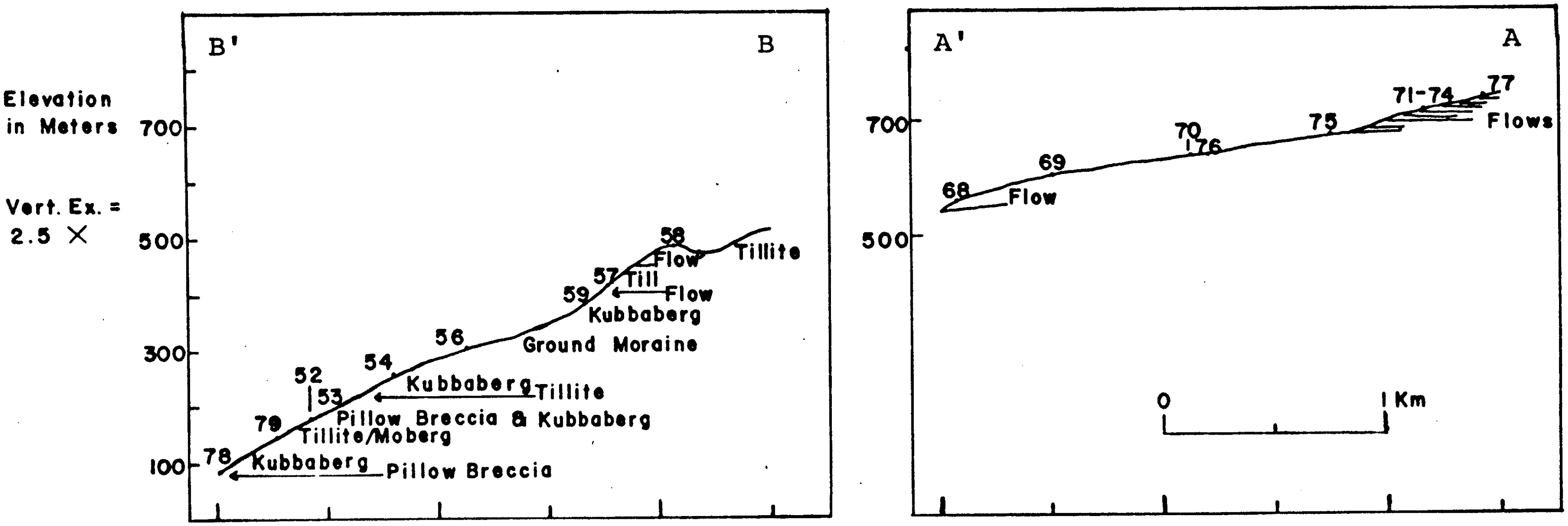
B'
B
Elevation in Meters
700
500
300
100
Vert. Ex. = 2.5 ×
58
Flow
Tillite
57
Till
59
Flow
Kubbaberg
56
Ground Moraine
54
52
53
Kubbaberg
Tillite
Pillow Breccia & Kubbaberg
79
Tillite/Moberg
78
Kubbaberg
Pillow Breccia
A'
A
700
500
77
71-74
Flows
75
70
176
69
68
Flow
0
1 Km

Figure 4a.

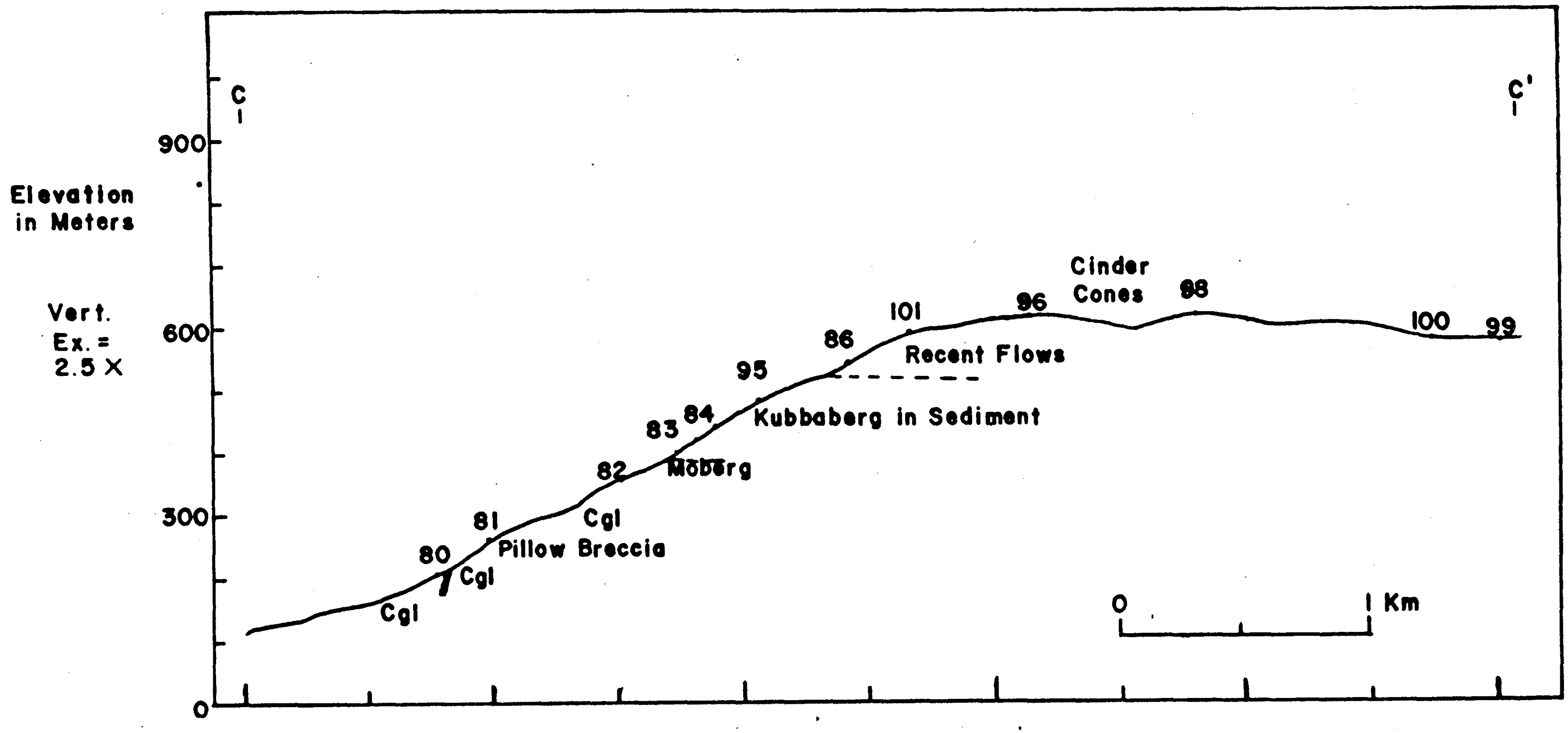
C
C'
900
600
300
0
Elevation in Meters
Vert. Ex. = 2.5 X
Cgl
80
Cgl
81
Pillow Breccia
Cgl
82
Moberg
83
84
95
Kubbaberg in Sediment
86
101
Recent Flows
96
Cinder Cones
98
100
99
0
1 Km

Figure 4b.

DISCUSSION OF RESULTS

In plotting all diagrams only the group averages were used. Not only does this make the diagrams more legible, it smooths out minor variations due to slight differences in percentages of phenocrysts in different samples.

With the oxides plotted against SiO_2 (Fig. 5) the continuity of the volcano becomes obvious. Most samples fall on a single trend; with the exception of most of the groups from Seljalandsfoss being slightly higher in Al_2O_3 and CaO, and slightly lower in Fe_2O_3 and TiO_2 (which is easily explained by the balance of plagioclase and magnetite phenocrysts), no one area is systematically different from the rest of the mountain. Unlike Hekla, which erupts basalts only on the flanks and andesites from the center of the volcano (Sigvaldason, 1974), some of the least silicic of all the basalts of Eyjafjöll are the top flows in the Seljavellir section, which are about as close as one can get to the central caldera. It is noted, however, that the acid rocks are only found in the moraines of debris coming from the central caldera.

There is a striking similarity between the most silicic (54% SiO_2) cinder blocks in the ash at Seljalandsfoss, samples 59 and 67, which probably represent dissected parts of flows at Seljavellir, and samples 108, 109, and 113 from the moraine at Falljökull on the north. The

Seljalands cinders and samples 59 and 67 are almost certainly from the same eruption. Both were subglacial or flooded by water (glacial melt) soon after eruption and represent the next-to-last subglacial eruption in their respective areas, which were once again covered by the glacier. The Falljökull samples are slightly different and, of course, their stratigraphic relationships are entirely unknown.

There is an apparent gap in composition between approximately 56 and 64% SiO_2. While it may be argued that the gap is only apparent because the more silicic rocks have not been well sampled and that with further sampling the gap would be filled, I do not believe this to be the case. Nine samples, representing every type observed in Falljökull moraine, were analyzed. Only three are acidic; the rest fall within the 47-56% SiO_2 range and are similar to other basalts analyzed. The fourth acidic rock, the least silicic of the group, is from the ground moraine at the top of Seljavellir. It comes from one of several large (.3-.5 m) angular fragments resembling the composite dikes found elsewhere in Iceland associated with central volcanoes. Few of the acidic rocks are pure; most have blebs of darker rock in them. This is common in composite dikes and is interpreted as the result of the coexistence of acid and basic melts, though how these melts are generated is the subject of debate (Walker, 1963; Walker and Skelhorn, 1966;

Baldridge et al., 1973).

The acid rocks (which had been hand-picked to eliminate visible basic fragments during grinding) do not always fall on the trends for the basalts on the SiO_2 plots. In most cases there is a break in slope, especially noticeable for TiO_2, MgO, and Na_2O. This could indicate either a change in precipitating phases or a different source material. Sample 111, at 65% SiO_2 is usually out of line with all the rest.

ALKALI VS. SiO_2

On a plot of total alkalis vs. SiO_2 (Fig. 6), most of the samples fall on the alkali side of the Hawaiian dividing line (MacDonald and Katsura, 1964). Six Heimaey samples (Thorarinsson et al., 1973) have been plotted for comparison: the 1973 eruption is represented by the samples highest is SiO_2 and alkalis, while the two samples lower in SiO_2 represent prehistoric eruptions.

The most recent eruptions of Eyjafjöll are among the highest in SiO_2 and it is interesting to note that they are almost the only ones to plot on the tholeiitic side of the Hawaiian dividing line. This is directly opposite from the findings of Carswell (1978) on Solheimajökull. That study indicates an increase in alkalis toward the top of

Fimmvorduhals, between Eyjafjallajökul and Myrdalsjökull. There is clearly not an overall increase in alkalis with time on Eyjafjöll, and there may have been a decrease. In addition to the recent eruptions above Sydstamörk, the most recent flows at Seljalands and Seljavellir are among the lowest in alkalis/SiO_2. (They are also among the least silicic.)

Sample 62 also plots on the tholeiitic side of the Hawaiian dividing line, but its silica and alkali content have probably been changed by hydrothermal alteration. Spherules of secondary mineralization, probably zeolites, on the order of .5-1 mm in diameter can be seen in hand sample.

Throughout the entire history of the mountain, most of the rocks fall within Jakobsson's (1972) transitional alkali basalt category.

The normative compositions indicate, however, that there has been an increase in silica saturation with the most recent eruptions. Two of the last four eruptions at Seljavellir are quartz normative, as are the last four eruptions at Sydstamörk (including sample 93). The quartz normative group at Seljalands is considered to represent the eruption producing samples 59 and 67, and is included in the Seljavellir count. The only other quartz normative rocks analyzed are two dikes and the rhyolites, all of unknown age.

Figure 7 shows the normative compositions plotted on a quartz-diopside-hypersthene-olivine-nepheline diagram.

The AFM diagram (Fig. 8) shows most clearly the relationships among the various compositions. It will be discussed in the section of fractionation.

Figure 5. Variation diagrams of oxides vs. SiO_2.

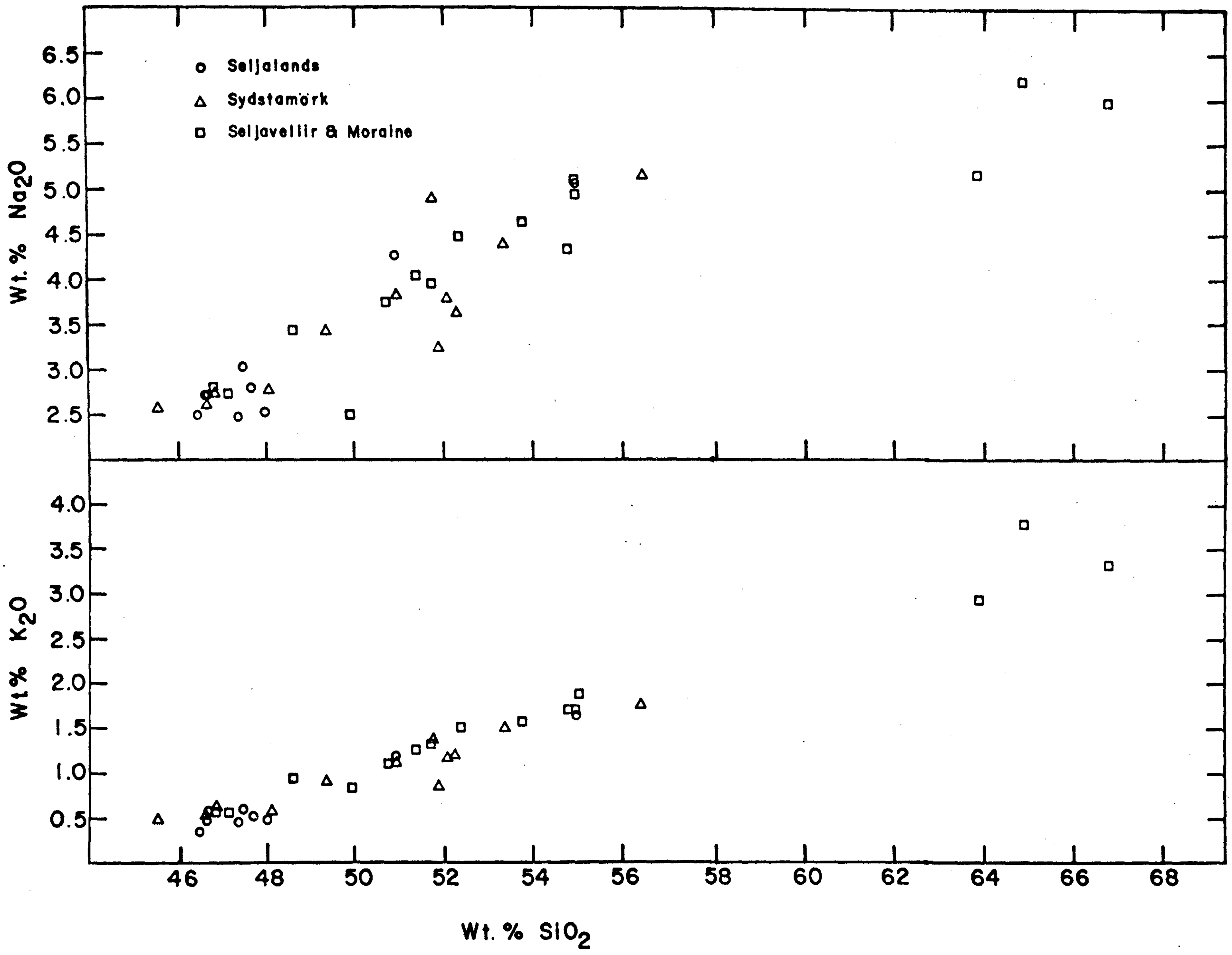

○ Seljalands
△ Sydstamörk
□ Seljavellir & Moraine
Wt.% Na$_2$O
6.5
6.0
5.5
5.0
4.5
4.0
3.5
3.0
2.5
Wt% K$_2$O
4.0
3.5
3.0
2.5
2.0
1.5
1.0
0.5
46
48
50
52
54
56
58
60
62
64
66
68
Wt.% SiO$_2$

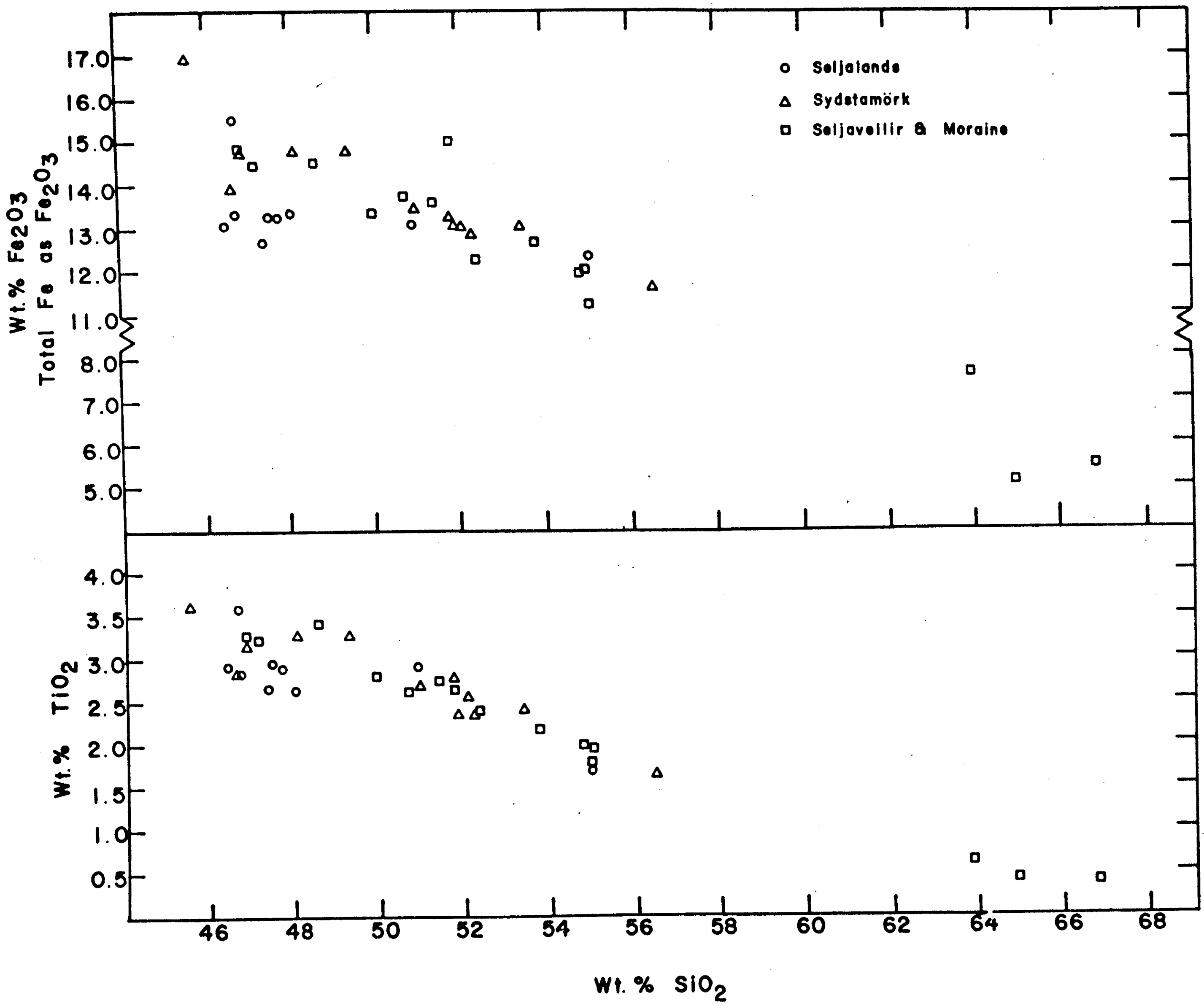

17.0
16.0
15.0
14.0
13.0
12.0
11.0
8.0
7.0
6.0
5.0
Wt.% Fe2O3
Total Fe as Fe2O3
○ Seljalands
△ Sydstamörk
□ Seljavellir & Moraine
4.0
3.5
3.0
2.5
2.0
1.5
1.0
0.5
Wt.% TiO2
46
48
50
52
54
56
58
60
62
64
66
68
Wt. % SiO2

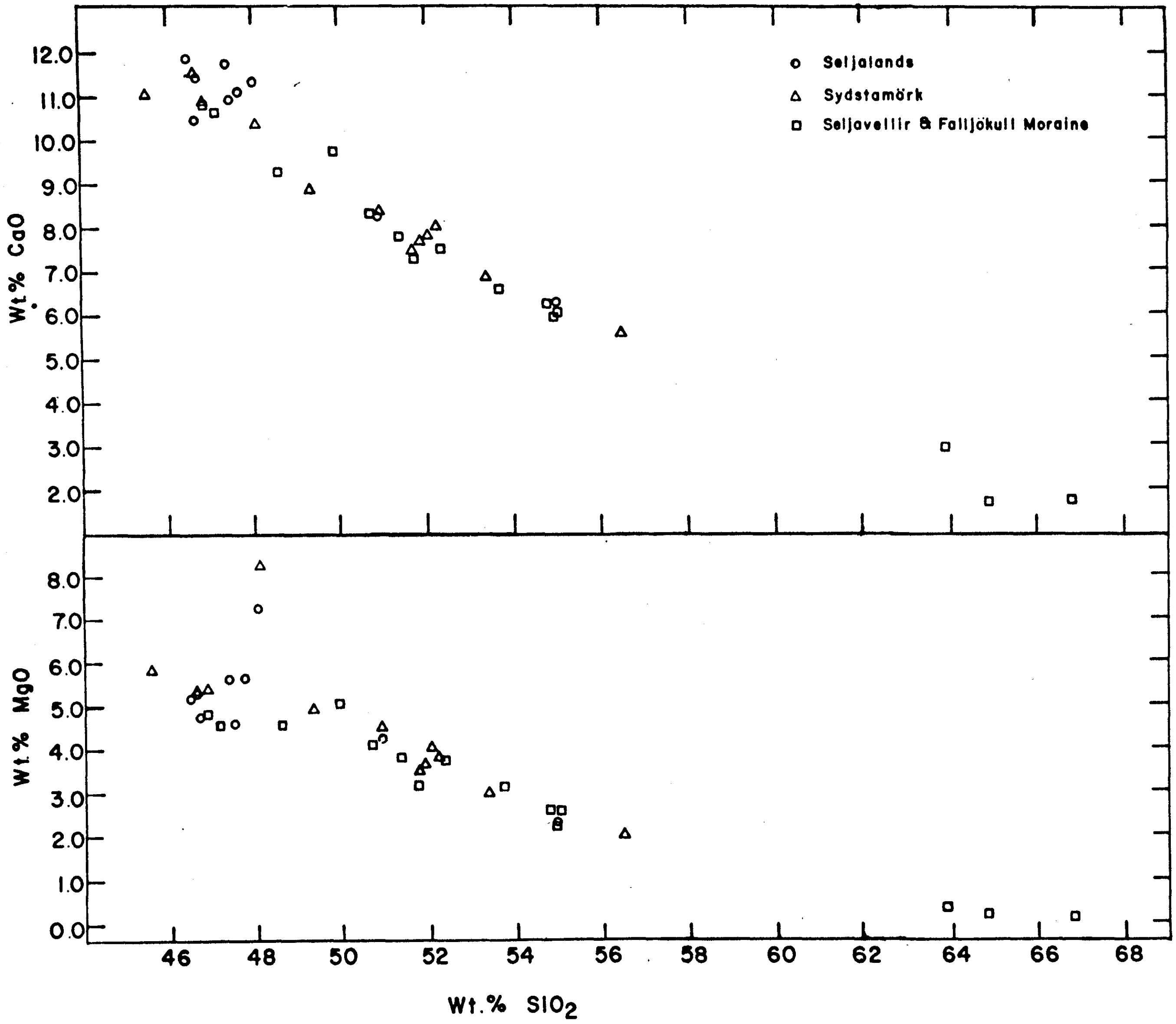
○ Seljalands
△ Sydstamörk
□ Seljavellir & Falljökull Moraine
Wt.% CaO
12.0
11.0
10.0
9.0
8.0
7.0
6.0
5.0
4.0
3.0
2.0
Wt.% MgO
8.0
7.0
6.0
5.0
4.0
3.0
2.0
1.0
0.0
46
48
50
52
54
56
58
60
62
64
66
68
Wt.% SiO_2

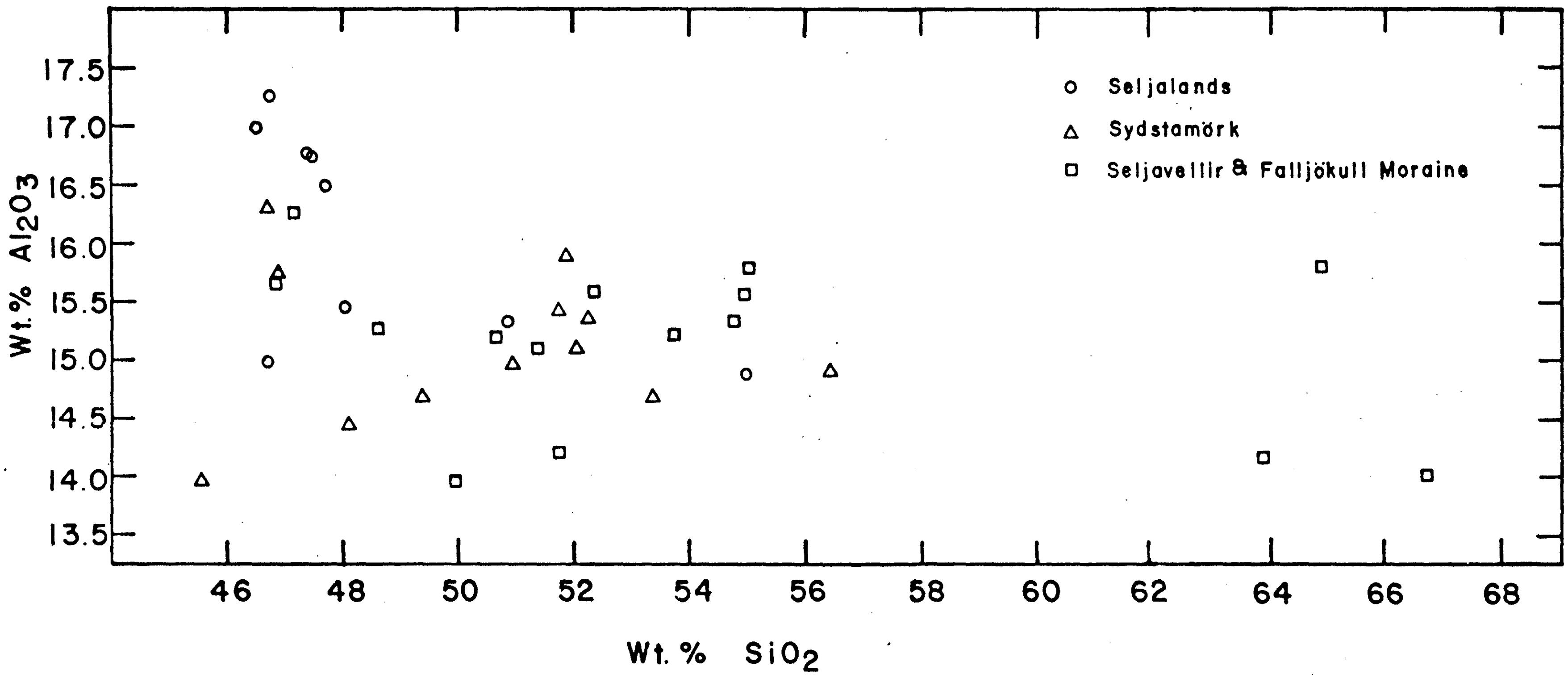

Seljalands
Sydstamörk
Seljavellir & Falljökull Moraine
17.5
17.0
16.5
16.0
15.5
15.0
14.5
14.0
13.5
Wt.% Al_2O_3
46
48
50
52
54
56
58
60
62
64
66
68
Wt.% SiO_2

Figure 6. Alkali vs. silica diagram showing Hawaiian dividing line after MacDonald and Katsura (1964). Analyses of Heimaey samples (Thoainsson _et_ _al_., 1973) designated by H.

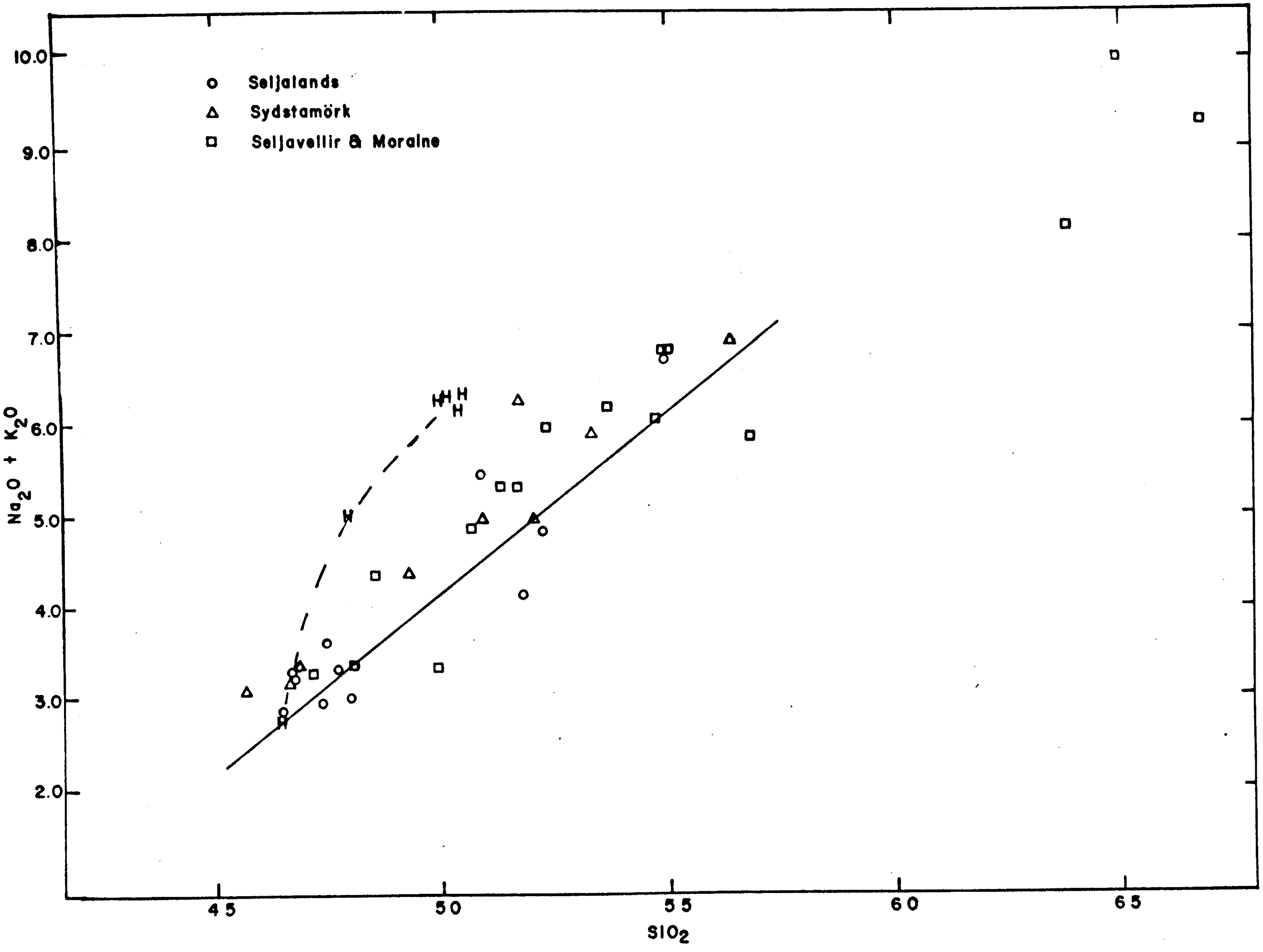
○ Seljalands
△ Sydstamörk
□ Seljavellir & Moraine
10.0
9.0
8.0
7.0
6.0
5.0
4.0
3.0
2.0
$Na_2O + K_2O$
45
50
55
60
65
SiO_2
H
H
H
H
H
H

Figure 7. Plot of normative compositions on Qz-Di-Hy-Ol-Ne diagram.

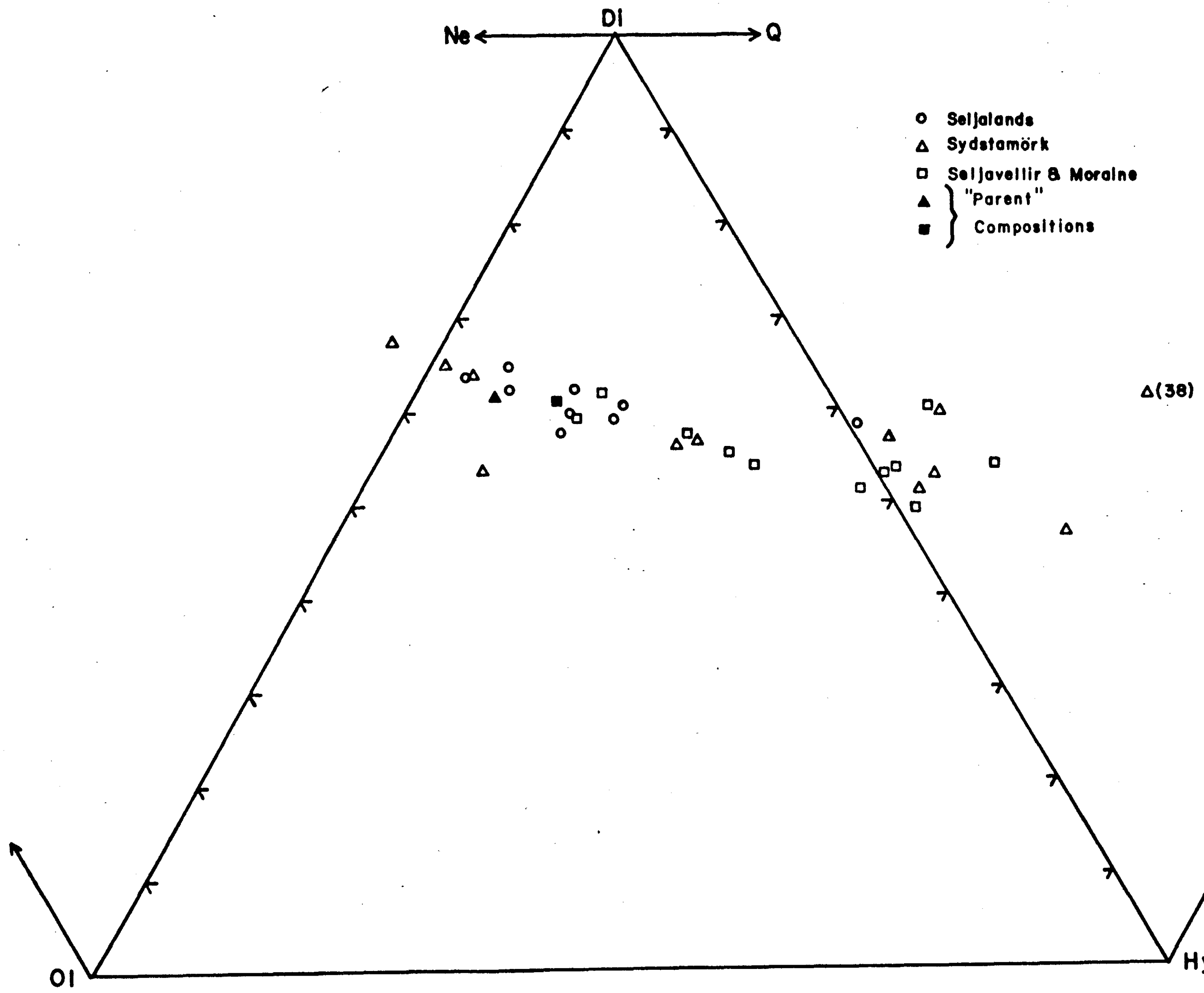
Ne
Di
Q
○ Seljalands
△ Sydstamörk
□ Seljavellir & Moraine
▲ "Parent"
■ Compositions
△(38)
Ol
Hy

Figure 8. Group compositions plotted on AFM diagram. Also indicated are the Thingmuli trend (Carmichael, 1964), Hawaiian alkali and tholeiite trends (MacDonald and Katsura, 1964), and Heimaey analyses (Thorarinsson, 1973).

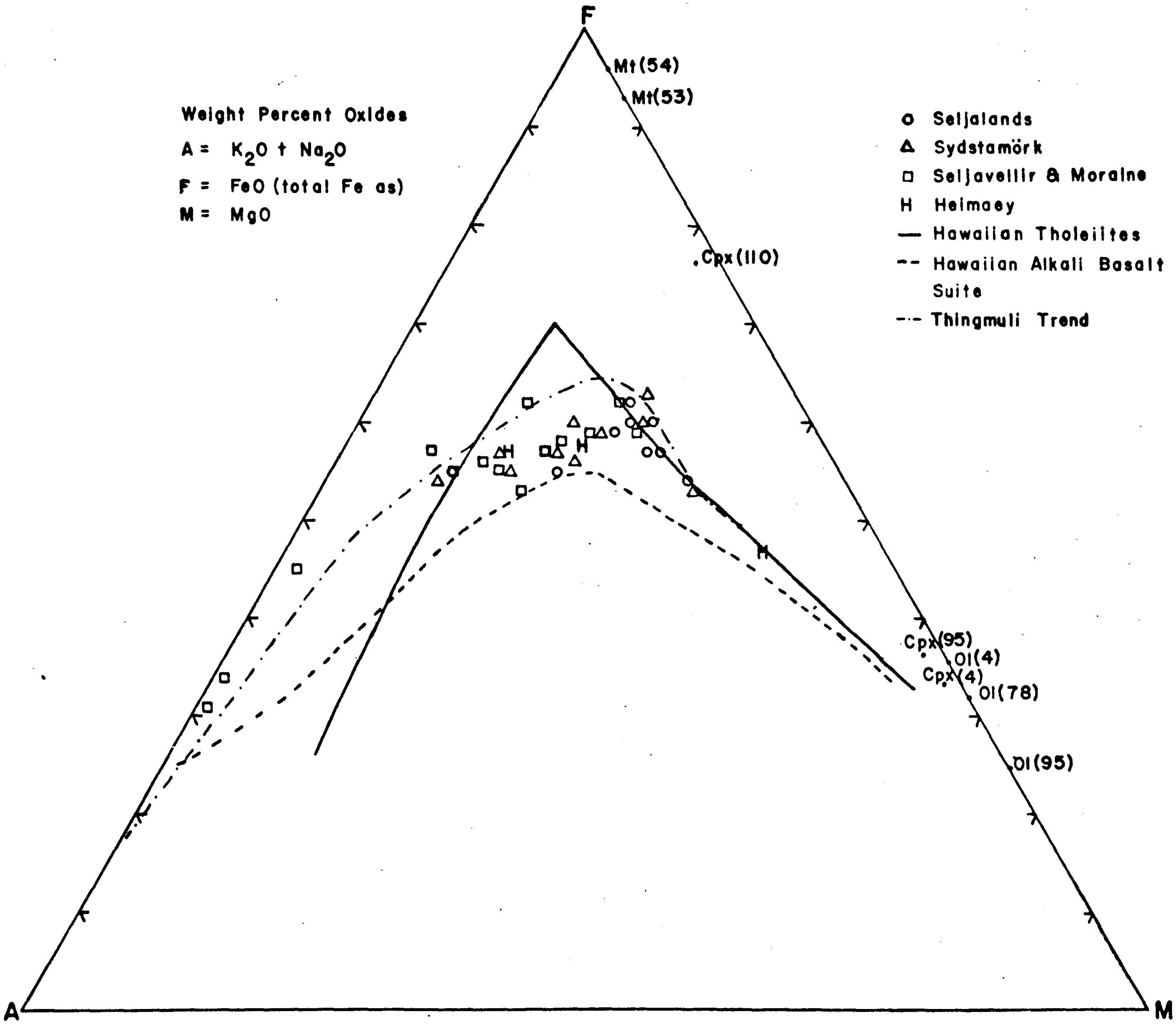
Weight Percent Oxides
A = K2O + Na2O
F = FeO (total Fe as)
M = MgO
F
A
M
Mt(54)
Mt(53)
Cpx(110)
Cpx(95)
Ol(4)
Cpx(4)
Ol(78)
Ol(95)
o Seljalands
△ Sydstamörk
□ Seljavellir & Moraine
H Heimaey
— Hawaiian Tholeiites
-- Hawaiian Alkali Basalt Suite
-·- Thingmuli Trend

MICROPROBE ANALYSES

Phenocrysts from representative samples were analyzed on the automated MAC-5 electron microprobe at M.I.T. Standard operating conditions were: accelerating voltage, 15 kv; beam current 30 na; count time 30 seconds or 60,000 counts. A variety of synthetic glasses and natural materials were used as standards. On-line data reduction was carried out using the GeoLab program of Finger and Hadadiacos (1972) which uses the correction procedures of Bence and Albee (1968) and Albee and Ray (1970). Results are shown in Table VI. Multiple analyses were made of each grain (2-15, usually 5) and the average of the analyses for each grain is given. In cases of zoned minerals, two or three analyses were made in each zone. In the interest of brevity, where the change in composition was gradational, or the zoning was complex, only the two extremes are given and are reported as center and edge. Some crystals, described as rimmed, consisted of only a center zone and a rim of a different composition.

Most rocks show a range of phenocryst composition. Samples 4 and 92 are both extremely porphyritic and also contain glomerocrysts of plagioclase and plagioclase plus augite. The olivines and pyroxenes in these rocks have a more constant composition than in other samples. The plagioclases, however, are even more zoned and embayed than in most other rocks.

Olivines have the most constant chemistry of all the phenocrysts, ranging from Fo_{74} to Fo_{84} in the basalts. It is interesting to note that the most magnesian olivines (Fo_{83-84}) occur in sample 95 (which contains nearly 50% SiO_2), where they cannot possibly be in equilibrium. The other Fo_{84} olivine analyzed is a resorbed phenocryst in sample 82. The rest of the olivines are Fo_{74-79}, the smaller, more euhedral ones being less magnesium. No olivines were observed in the intermediate rocks (SiO_2 content 53-56%), but an altered olvine of Fo_{11} was analyzed from sample 77. The olivines are mostly subhedral and slightly rounded, but the more silicic basalts (50-52% SiO_2) contain fragments as well. Sample 3 contains olivine rimmed with pyroxene (analyses below, picture in Fig. 10a).

Sample 3, point 2	olivine	pyroxene rim
SiO_2	39.49	49.89
Al_2O_3	-	4.74
FeO	19.73	6.71
MgO	42.01	15.49
CaO	.34	20.84
Na_2O	-	.35
TiO_2	-	1.04
MnO	.29	.13
NiO	.18	-

Clinopyroxene analyses vary considerably, both within a single thin section and between samples. No orthopyroxene was observed. The pyroxenes in the basalts are augite and diopsidic augite; those in the acid rocks are ferroaugite. Though CaO holds relatively constant, from $Ca_{.78}$ to $Ca_{.85}$ per 6-oxygen formula unit, FeO, MgO, and Al_2O_3 vary considerably. The Na_2O content is uniformly low, and TiO_2, while variable, is less than expected: 0.9-2.4 weight % in the augites and diopsidic augites. Though these rocks contain no normative nepheline, they plot on the alkali side of the Hawaiian dividing line in the silica vs. alkali diagram, and their mineralogy is that of alkali basalts (plagioclase, augite, olivine, magnetite, and ilmenite with no orthopyroxene (Wilkinson, 1967).

In thin section the pyroxenes appear as beige euhedral crystals and crystal fragments in the basalts and as green euhedral crystals intergrown with euhedral magnetites in the more acid rocks. Many are zoned or rimmed (see Figure 10b) and a few are sector-zoned. Usually the groundmass pyroxenes are too small to analyze, but compositions of two from sample 82, which is coarser-grained, are given in Table VI. As could be expected, the groundmass pyroxenes are more iron-rich than the phenocrysts; the average composition of the groundmass pyroxene is close to the composition of the rim of the phenocryst listed as point 1 in Table VI. Pyroxene compositions are plotted in Figure 9.

The magnetite and ilmenite analyses showed where the TiO_2 was. It had been noted in thin section that many samples contained groundmass ilmenite needles. The analyses showed that some of the square, rounded, or fragmented oxide phenocrysts were also ilmenite, not magnetite. Unfortunately, the groundmass needles were all too small to analyze; only the ilmenite from sample 82 was a blocky one. The analyses of point 1 from sample 4 show that the magnetite may also be zoned, though it is unknown how many are.

All the magnetites from the basalts (up to 52% SiO_2) are titaniferous, and the smaller phenocrysts and groundmass magnetite are more so than the larger phenocrysts. Magnetite phenocrysts are not abundant, at most 3 or 4 in a thin section, but magnetite is abundant in the groundmass. No magnetite associated with the green pyroxene in the silicic rocks has yet been analyzed.

The plagioclases in all the basalts are zoned, resorbed, and embayed (see Figure 10c). The zoning may be normal, reverse, or oscillatory. In sample 4, all three types occur in the same thin section. The compositions vary from An_{46} to An_{81} in the basalts. Zoning is not absolutely symmetric but is usually approximately so. The last page of Table VI shows in more detail the zoning in a single plagioclase crystal from sample 4. The variation of Ca and Na is shown schematically in the sketch below the analyses. The transitions between zones are probably more abrupt and not gradual as shown, but no continuous scan was made and the sketch is based on analyses of discrete zones. Many of the plagioclases have glass inclusions which, when analyzed, give the composition of the surrounding plagioclase.

Sample 93 at 56.47 weight % SiO_2 is the most silicic of the compositions on the low side of the silica gap. It is also the least well crystallized, containing plagioclase phenocrysts in a glassy matrix. The composition of its plagioclase is An_{40-46}.

Sample 110 is the rhyolite chosen for phenocryst analyses because it is the freshest. There is virtually no compositional variation or zoning in its plagioclase phenocrysts. All are oligoclase with no sign of more acid rims. The phenocrysts have somewhat blurred twinning and gradual extinction, but most have fairly sharp edges.

The groundmass plagioclase of all samples is too small to analyze by microprobe.

Figure 9. Clinopyroxene compositions plotted on a CFM diagram.

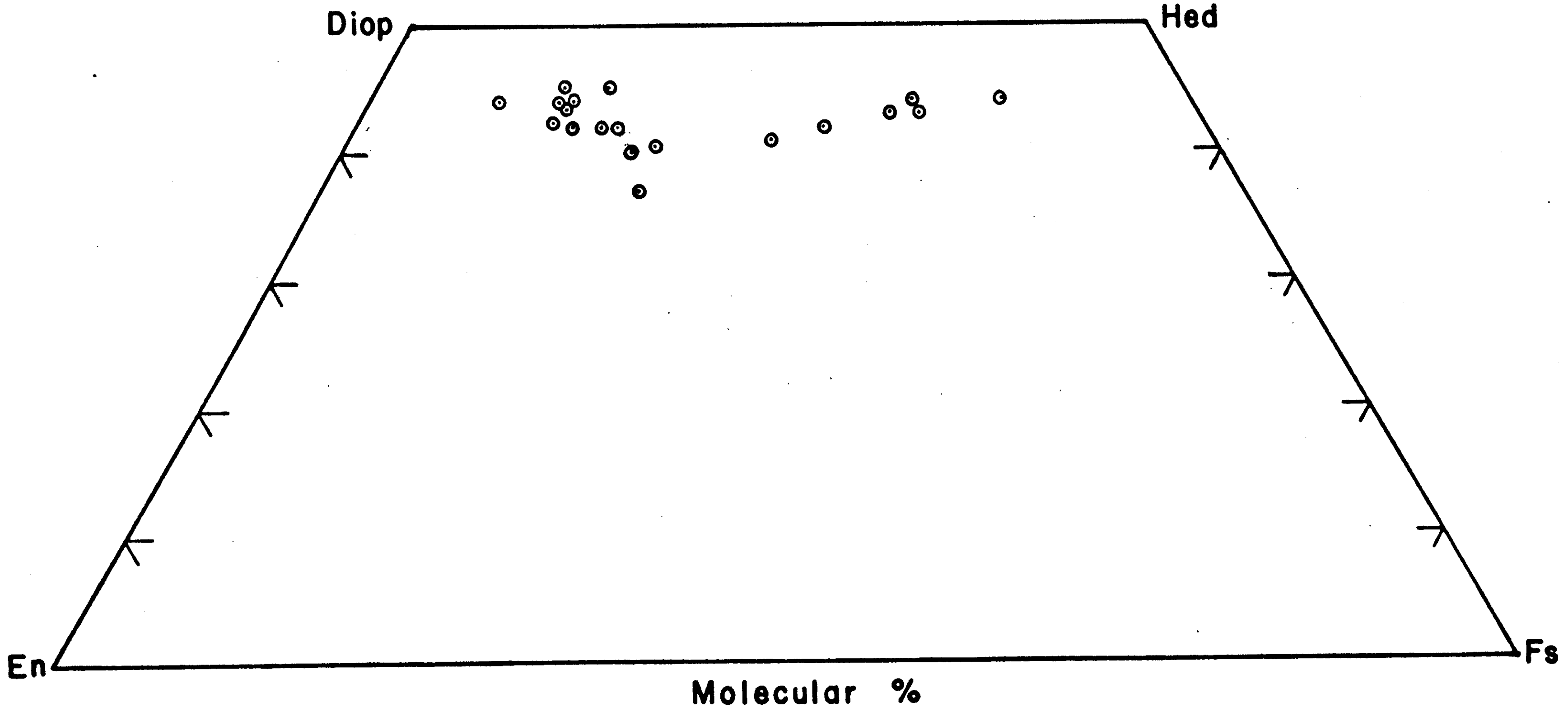
Diop
Hed
En
Fs
Molecular %

TABLE VI. MICROPROBE ANALYSES

Olivine Analyses from Representative Samples

Sample Number	4	4	92	92	3	3	82	82	82*
Grain Description		pt. 5	prismatic	pt. 3	pt. 1	pt. 2 rim on olivine	micro-phenocryst	pt. 6	pt. 2
SiO_2	38.42	38.65	38.75	39.17	39.05	39.49	38.31	39.59	38.66
FeO^1	22.90	22.07	22.89	19.45	21.29	19.73	24.05	20.31	22.47
MgO	40.34	40.08	38.42	41.05	40.95	42.01	38.65	41.90	39.88
CaO	.26	.30	.28	.30	.28	.34	.29	.42	.42
MnO	.34	.27	.32	.23	.25	.29	.36	.25	.30
NiO	.14	.09	.12	.12	.07	.18	.10	.13	.07
Total	102.40	101.46	100.78	100.32	101.89	102.04	101.76	102.60	101.80
Si	.980	.990	1.009	1.003	.991	.994	.988	.993	.988
Fe	.489	.473	.498	.416	.452	.415	.518	.425	.480
Mg	1.535	1.530	1.492	1.567	1.550	1.577	1.486	1.566	1.521
Fo	.76	.76	.75	.79	.77	.79	.74	.79	.76

* Designates phenocryst compositions used in fractionation modeling.

TABLE VI. (cont.)

Olivine Analyses from Representative Samples

Sample Number	82	95	95	78*	78	77
Grain Description	pt. 3	pt. 1	pt. 5	pt. 2	pt. 1	very altered prismatic
SiO_2	39.92	39.75	38.18	39.43	38.88	30.54
FeO[1]	16.02	15.17	16.54	19.83	22.21	61.73
MgO	45.68	46.02	43.98	42.12	39.87	4.20
CaO	1.61	.32	.28	.23	.42	.43
MnO	.20	.23	.18	.24	.28	2.05
NiO	.10	.23	.10	.15	.16	---
Total	103.53	101.72	99.26	102.00	101.82	98.95
Si	.978	.984	.977	.992	.993	1.005
Fe	.328	.314	.354	.417	.473	1.701
Mg	1.670	1.700	1.677	1.581	1.517	.206
Fo	.84	.84	.83	.79	.76	.11

* Designates phenocryst compositions used in fractionation modeling.

TABLE VI. (cont.)

Magnetite and Ilmenite Analyses from Representative Samples

Sample Number	4	4	82	82*	53*	54	54	78	78
Grain Description	pt. 1 center	pt. 1 rim	ground magnetite	ground ilmenite	pt. 2 (lg)	pt. 3 (lg)	pt. 1 euhedral	square subhedral	rounded ilmenite
SiO_2	.10	.16	.11	.02	.05	.10	.11	.09	.06
Al_2O_3	6.01	3.83	1.47	.14	4.76	4.75	3.11	2.74	.42
FeO	59.69	61.36	65.20	44.07	66.07	65.77	64.95	65.84	43.53
MgO	5.12	4.73	1.43	1.63	5.19	5.00	2.94	4.02	4.30
TiO_2	17.90	20.74	26.18	50.81	17.51	17.96	22.74	21.82	49.11
MnO	.44	.43	.54	.61	.35	.33	.45	.59	.58
NiO	.05	.03	0	.01	.04	.02	0	.05	.03
Cr_2O_3	5.95	3.78	.12	.03	.32	.97	.59	.09	0
V_2O_5	.97	1.25	1.09	.69	.78	.91	.99	.70	.77
Total	96.23	96.31	96.14	98.01	95.07	95.81	95.88	95.94	98.80

* Designates phenocryst composition used in fractionation modeling.

TABLE VI. (cont.)

Clinopyroxene Analyses from Representative Samples

Sample Number	82*	82	82	82	54	54	95	95	78
Grain Description	pt. 1 rimmed center	pt. 1 phenocryst rim	ground-mass	ground-mass	pt. 1 zoned phen. center	pt. 1 rim	2	7	pt. 3
SiO_2	50.21	50.86	47.19	51.44	51.16	49.39	51.03	49.21	51.07
Al_2O_3	4.00	2.36	5.94	1.98	2.65	4.30	3.97	5.02	2.36
FeO	7.91	10.55	9.56	11.29	8.22	8.59	5.81	8.33	9.06
MgO	14.52	14.00	13.16	13.93	15.32	14.09	16.05	14.18	14.79
CaO	21.23	19.79	20.93	20.19	20.37	20.72	21.14	20.70	20.20
Na_2O	.43	.31	.43	.38	.33	.39	.29	.46	.40
TiO_2	1.44	1.40	2.43	1.39	1.13	1.88	.89	1.61	1.06
MnO	.14	.20	.13	.22	.19	.19	.06	.18	.30
Total	99.88	99.47	99.77	100.82	99.37	99.55	99.24	99.69	99.24
Fe	.244	.332	.301	.351	.256	.268	.179	.259	.284
Mg	.803	.785	.739	.773	.851	.786	.884	.789	.827
Ca	.845	.798	.846	.805	.814	.830	.837	.827	.812
Al	.174	.103	.263	.087	.116	.189	.172	.220	.104

* Designates phenocryst compositions used in fractionation modeling

TABLE VI. (cont.)

Clinopyroxene Analyses from Representative Samples

Sample Number	4	92	93	93	93	93*	77	77
Grain Description	pt. 1	pt. 2	green center	toward edge	beige outer zone	pt. 5 cluster	beige	green
SiO_2	49.29	49.78	50.13	50.01	51.51	50.23	48.91	48.48
Al_2O_3	4.45	3.96	1.01	1.13	1.49	1.37	.82	.78
FeO	7.76	8.01	19.21	17.55	13.10	13.43	22.11	24.24
MgO	15.05	15.21	8.62	9.98	13.03	12.60	6.22	4.18
CaO	21.48	21.14	19.61	19.25	19.25	19.41	19.24	19.43
Na_2O	.39	.49	.30	.38	.37	.36	.34	.38
TiO_2	1.38	1.73	.46	.54	.59	.60	.34	.44
MnO	.13	.15	.73	.75	.50	.48	.80	.76
Total	99.93	100.47	100.07	99.59	99.84	98.48	98.78	98.69
Fe	.241	.247	.627	.571	.414	.433	.744	.825
Mg	.832	.836	.501	.579	.735	.725	.373	.253
Ca	.854	.836	.821	.803	.781	.802	.829	.848
Al	.193	.171	.045	.051	.065	.062	.038	.037

* Designates phenocryst compositions used in fractionation modeling.

TABLE VI. (cont.)

Clinopyroxene Analyses from Representative Samples

Sample Number	110	110	110*
Grain Description	pt. 1 zoned tan center	pt. 1 green rim	small green
SiO_2	49.86	48.89	49.52
Al_2O_3	2.27	.61	.71
FeO	12.23	20.22	21.27
MgO	13.99	6.57	6.25
CaO	18.84	18.98	19.49
Na_2O	.63	.54	.44
TiO_2	.90	.31	.33
MnO	.52	.99	.89
Total	99.24	97.11	98.90
Fe	.392	.688	.711
Mg	.772	.398	.372
Ca	.789	.827	.834
Al	.104	.029	.033

* Designates phenocryst compositions used in fractionation modeling.

TABLE VI. (cont.)

Plagioclase Analyses from Representative Samples

Sample Number	4*	4	92	92	82	82	73	73	73	73
Grain Description	core of zoned	micro-pheno.	pt. 6 core	pt. 6 rim	pt. 4	small euhed.	pt. 1 rim	next band in	glass	core
SiO_2	48.50	53.95	52.65	50.59	47.74	53.05	50.08	48.01	46.32	46.93
Al_2O_3	31.93	28.82	28.35	30.36	33.38	29.92	31.31	32.61	32.73	33.12
FeO	.65	.88	.71	.88	.67	.84	.73	.67	.67	.63
MgO	.09	.15	.12	.10	.09	.16	.12	.11	.11	.10
CaO	16.84	11.83	13.18	14.94	16.42	12.03	14.56	16.02	16.44	16.35
Na_2O	2.46	4.71	4.56	3.75	2.09	4.30	3.11	2.51	2.32	2.30
K_2O	.07	.26	.17	.18	.07	.23	.12	.06	.06	.07
MnO	.04	.00	.05	.04	.01	.02	.03	.07	.06	.06
TiO_2	.06	–[1]	.11	.14	–[1]	–[1]	.11	.04	.07	.05
	100.64	100.60	99.90	100.98	100.47	100.55	100.17	100.10	98.78	99.61
Si	2.206	2.442	2.400	2.281	2.183	2.403	2.286	2.196	2.161	2.171
Al	1.712	1.537	1.523	1.628	1.799	1.596	1.683	1.764	1.799	1.805
Ca	.822	.573	.643	.725	.803	.583	.711	.786	.821	.810
Na	.271	.413	.403	.328	.185	.377	.274	.223	.209	.205
An	79	58	61	69	81	61	72	78	80	80

[1] Not determined.

* Designates phenocryst compositions used in fractionation modeling.

TABLE VI. (cont.)

Plagioclase Analyses from Representative Samples

Sample Number	73	78	78	78	98	98	110
Grain Description	pheno.	pt. 4 center	rim	glass	pt. 4	groundmass	pt. 5
SiO_2	49.42	48.45	55.53	49.53	56.45	57.94	66.06
Al_2O_3	31.50	32.46	27.51	32.49	27.34	25.65	21.20
FeO	.71	.67	.72	.68	.58	.72	.26
MgO	.11	.11	.11	.10	.06	.05	.00
CaO	15.22	15.03	9.48	14.19	9.62	8.16	2.45
Na_2O	2.67	2.66	5.85	2.58	5.97	6.62	9.61
K_2O	.09	.09	.33	.09	.25	.35	1.11
MnO	.00	.01	.00	.02	.01	.00	.00
TiO_2	.07	–[1]	–[1]	–[1]	–[1]	–[1]	–[1]
	99.79	99.48	99.53	99.68	100.28	99.49	100.69
Si	2.267	2.229	2.516	2.275	2.527	2.614	2.895
Al	1.703	1.759	1.469	1.759	1.442	1.364	1.095
Ca	.747	.740	.460	.698	.462	.395	.114
Na	.237	.236	.513	.228	.520	.579	.817
K					.014	.019	.061
An	76	76	47	75	46	40	11

[1] Not determined.

* Designates phenocryst compositions used in fractionation modeling.

SLIDE 4. Zoned plagioclase, core-out, 1 analysis each zone, except first two are both **center.**

SiO	48.24	48.75	51.12	53.00	49.66	52.32	51.60	51.57	52.46
Al_2O_3	31.88	31.97	30.46	28.91	31.07	28.81	29.90	29.94	28.63
CaO	16.81	16.87	14.81	13.14	15.62	13.29	14.53	14.38	13.30
Na_2O	2.61	2.31	3.45	4.13	2.85	3.88	3.55	3.71	4.19
K_2O	.08	.06	.12	.13	.07	.14	.09	.10	.18
FeO	.63	.67	.67	.67	.73	.70	.67	.76	.74
MgO	.08	.10	.11	.13	.10	.13	.12	.13	.14
NiO_2	-	.02	-	.05	-	-	-	.07	-
MnO	.03	.04	.02	.01	.05	.03	-	.02	.03
TiO_2	.07	.04	.08	.08	.06	.11	.09	.07	.14
	100.43	100.87	100.84	100.25	100.21	99.41	100.55	100.75	99.81
Si	2.215	2.226	2.320	2.405	2.274	2.396	2.345	2.341	2.397
Al	1.725	1.721	1.628	1.546	1.677	1.555	1.602	1.602	1.542
Ca	.826	.824	.719	.638	.766	.652	.707	.699	.650
Na	.231	.204	.302	.363	.252	.344	.312	.326	.370

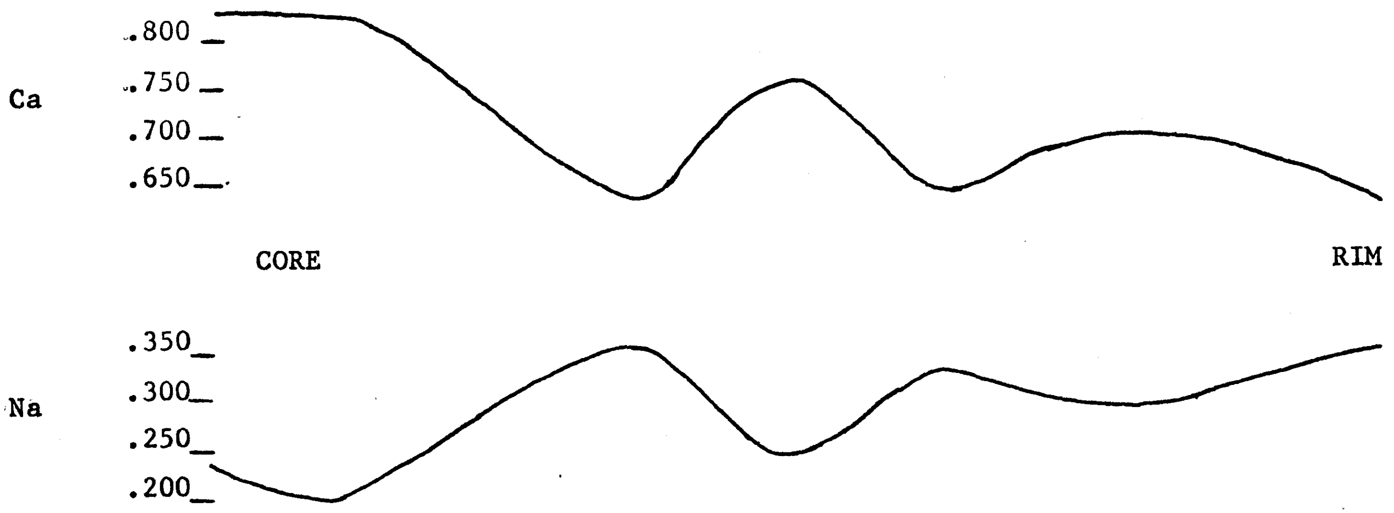

Figure 10. Photomicrographs of representative phenocrysts.

Figure 10a.

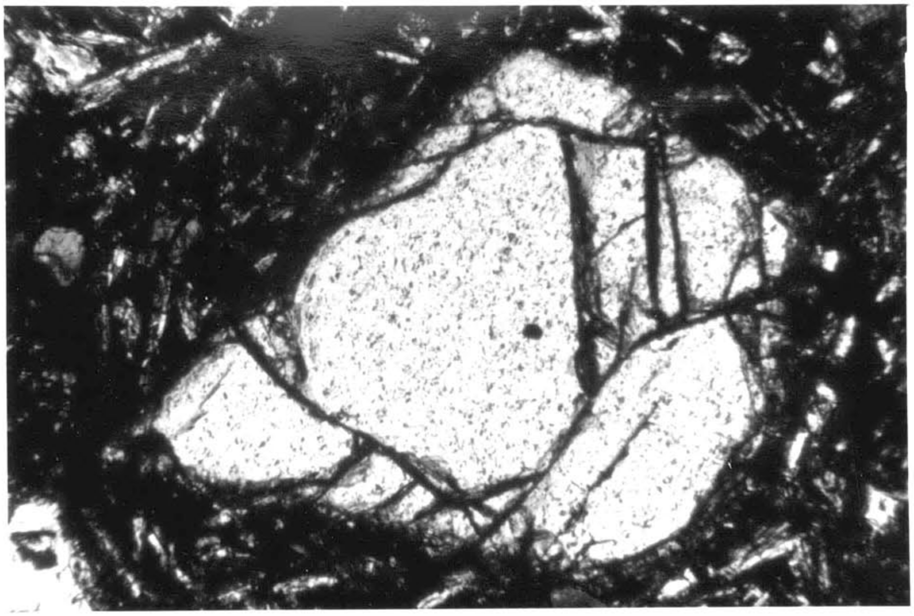

Olivine phenocryst. Sample 82, pt. 2.

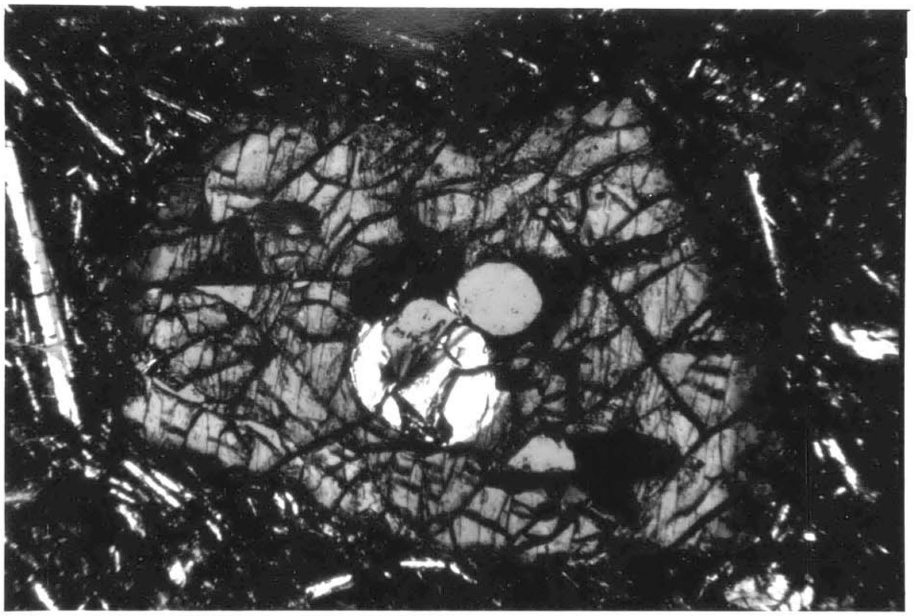

Olivine rimmed with pyroxene (x nicols). Sample 3, pt. 2.

Figure 10b.

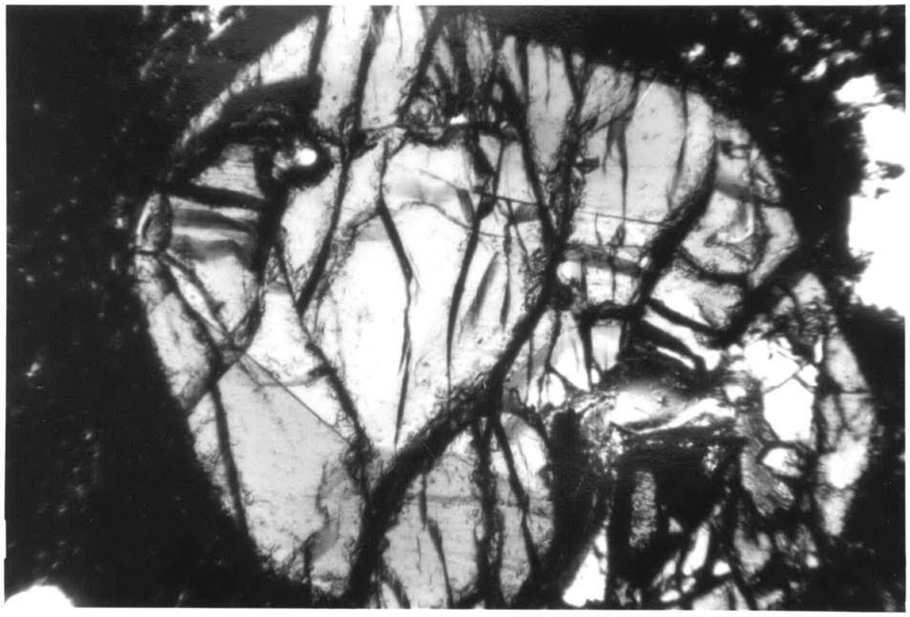

Zoned pyroxene. Sample 54, pt. 1.

Pyroxene. Sample 92, pt. 2

Figure 10c.

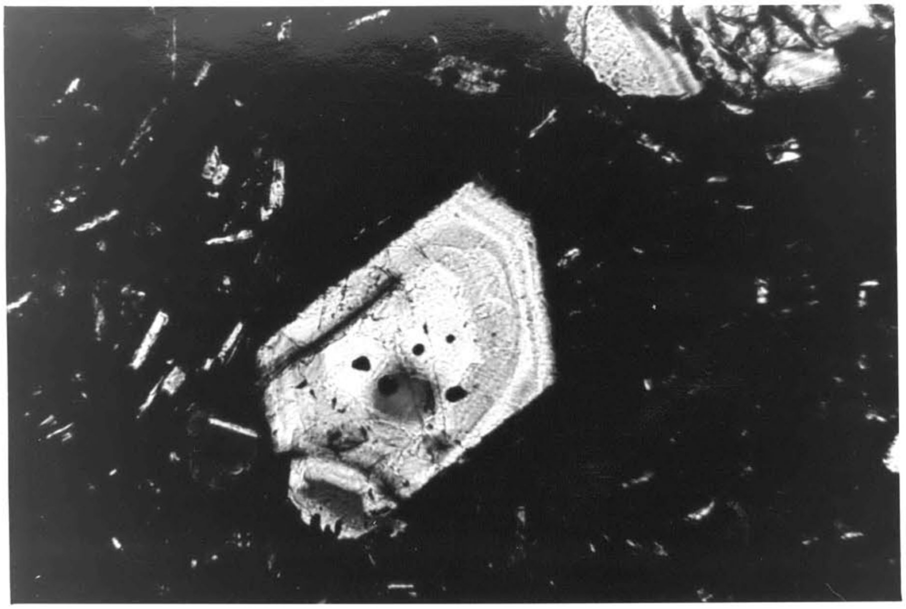

Zoned plagioclase. Sample 4 (see last page, Table VI).

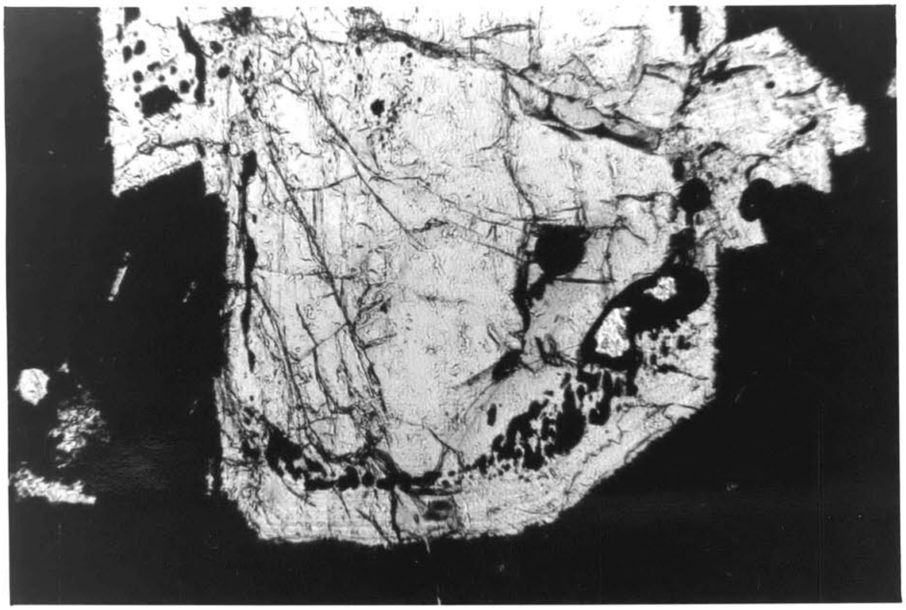

Plagioclase phenocryst with glass. Sample 73, pt. 1.

misnumbering of
pp. 90 thru 98

Figure 10d.

Typical resorbed plagioclase. Sample 81.

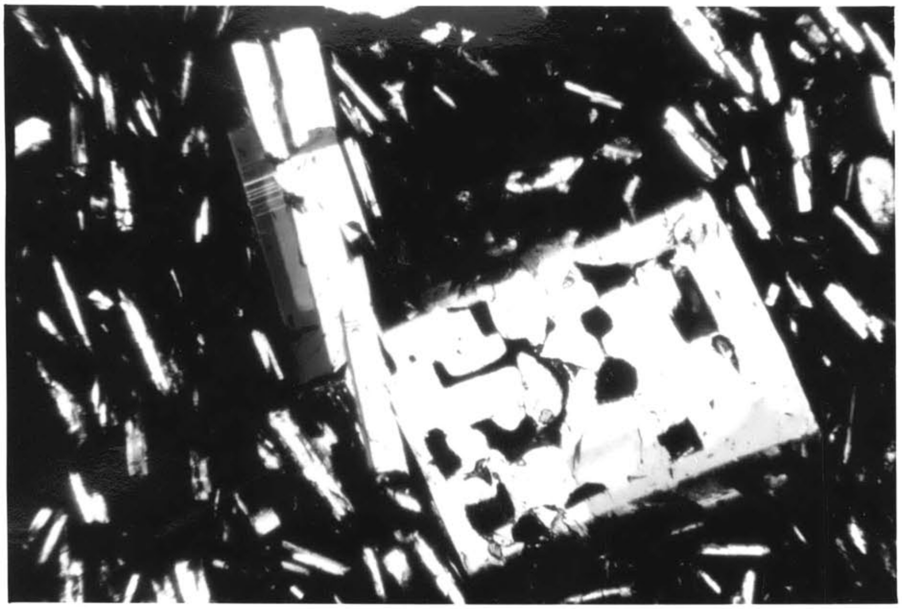

Plagioclase. Sample 93, pt. 4.

Pages 90-98 do not exist. A misnumbering error by the author.

EVIDENCE OF FRACTIONATION

It is evident from looking at the rocks that crystal/liquid fractionation has taken place. All of the basalts are porphyritic, and when viewed in thin section, many of the phenocrysts show evidence of disequilibrium with the surrounding rock. Almost all of the plagioclase phenocrysts are zoned. The pyroxenes in the basalts of lower SiO_2 content are euhedral and unzoned, but pyroxene from rocks with 50% or more SiO_2 are often fragmented, rimmed, or zoned. Most indicative of fractionation is the fact that phenocrysts of several different compositions may be found in one rock. The occurrence of the most magnesian olivine and pyroxene analyzed in a rock containing more than 50% SiO_2 also indicates that many of these phenocrysts have not formed from a melt represented by the bulk composition of the rocks they occur in, but must have crystallized at some depth from a more mafic melt. Probably turbulence connected with the eruption caused these phenocrysts to become entrained in the magma which was erupted.

The trends in chemical composition also indicate fractionation. Samples 4 and 92, because of their extremely high phenocryst content, do not fall on a line with the other samples on the SiO_2 plots, and plot closer to the MgO corner than any other samples on the AFM diagram (Fig. 8). The location of olivine and clinopyroxene on that diagram clearly show why samples 4 and 92 plot as they do, and support the contention that is separation of these phenocrysts from a more mafic primary melt which results in the compositions observed on Eyjafjöll.

FRACTIONATION MODELING

Ideally, of course, one works with aphanitic or glassy rocks which truly show the melt composition. Only one such sample, 93, out of more than 120 samples, was found on Eyjafjöll. Even it contains plagioclase and some clinopyroxene microphenocrysts. All the others are porphyritic and most of the basalts contain phenocrysts of olivine, augite, and plagioclase.

Clearly the whole rock analyses do not represent melt compositions, but rather melt plus phenocrysts. However, the phenocrysts contained are likely to be the ones which were fractionating out of the parent magma to obtain the new melt composition rather than from a completely unrelated melt, and therefore it should be possible to use the whole rock compositions for modeling purposes.

Comparison on the AFM diagram of the Eyjafjöll rocks with the composition of their olivines and clinopyroxenes and with the trends of suites from other areas reveals that none of these rocks represents what could be considered a primary melt. Considerable olivine and pyroxene have already been lost. Based on the actual compositions of phenocrysts plotted on the AFM diagram, the eruptions seem to begin in the middle of this fractionation sequence, when magnetite has started to precipitate and drive the compositions away from the iron-magnesium side toward the alkali corner.

In selecting a "parent" composition, then, it is recognized that this is not a true parent in the overall fractionation model, but an intermediate stage which might, with further fractionation, give rise to still more differentiated rocks. Several possible "parents" were considered, using these criteria: low SiO_2, low K_2O, and preferably not unusually high contents of any other oxide which might indicate addition of abundant phenocrysts to the starting melt. The compositions represented by samples 81 and 82 are very similar to the compositions of the flows 71-74 above Seljavellir. Since those were obviously not erupted subglacially, and 81, which is a pillow breccia, probably was, it was believed that these two sets of samples, 81 and 82, and 71-74, represent two separate eruptions. That would make it even more likely that they represent the least differentiated magma, coming from depth, while more silicic rocks were the result of various periods of residence in a magma chamber where they fractionated to various degrees.

Fractionation was modeled using the program of Doherty and Wright (1971). Sample 81 was chosen as a parent composition, and actual phenocryst compositions determined by microprobe were subtracted in an attempt to derive the more silicic rock compositions. Pure albite and pure anorthite were also supplied as possible phenecryst phases to allow the program to formulate its own plagioclase composition, as a wide variety of plagioclase compositions exist in the rocks.

The results were not as expected. The composition of 81 proved to be a satisfactory parent for some rocks, namely the late and post-glacial rocks near Sydstamörk, and the most recent flows at Seljavellir. (As previously mentioned 81 is nearly identical with flows 71-74 at Seljavellir.) However, it was soon seen that the K_2O and Na_2O contents of even the least silicic rocks (52, 53, 54, 61) of the lower sequence at Seljavellir could not be derived from fractionating the composition of 81.

A second attempt at modeling was made using the group average composition of samples 52, 53, 54, and 61 as a "parent". At more than 48% SiO_2 this average plots well into the Ol-Di-Hy field on the Ol-Di-SiO_2 face of the basalt tetrahedron, but it is the least silicic rock group at Seljavellir and also fairly near the base of the section.

The results of the second attempt at modeling fractionation show that nearly all the rocks at Seljavellir and some of the rocks at Sydstamörk can indeed be derived from the composition of group 52.

Agreement between the calculated derivative compositions and the observed group averages for Eyjafjöll rocks was determined by the sum of the squares of the differences. Any sum above .10 was not considered to fit, and possible reasons and/or implications are discussed below. Generally the sum was less than .05 (see Table VII for calculations).

A second criterion was that no single difference in weight % oxide should exceed .10 (for most oxides, or .15 for SiO_2 or Na_2O, as the precision of the analyses was less for these oxides). Any difference in weight % oxide between calculated composition and rock average composition greater than these limits is noted in the results in Table VII.

Except where noted in the discussion which follows, satisfactory results in each case were obtained with only one of the possible parents tried. Other calculations usually resulted in sums of the squares of the differences above the 0.10 cutoff limit and were always at least twice as great as the corresponding value for the accepted model.

Almost all the glacial rocks at Seljavellir can be derived from parent composition 52. The composition represented by samples 78 and 79 is an interesting exception. These samples are from radiating columns and kubbaberg, the lowest rocks in the Seljavellir section. Their SiO_2 content is 52.36%, higher than the group composition of group 52 (the proposed parent), which occurs above them in the section. The composition derived from fractionating that parent certainly is closer to that of 78 and 79 than is the composition derived from fractionating 81, but it is still too low in K_2O and Na_2O. (These are the same elements in which 52 is too rich to be derived by fractionating 81.) It is realized that these elements and TiO_2 are the most difficult major elements to match in a fractionation model, but nearly perfect matches between model-derived compositions and the actual compositions for other rocks (see Table VII) makes it difficult to accept differences of over .15 weight % for any oxide, especially those with such narrow limits of precision in analysis as K_2O and TiO_2.

There are two possible expanations for the failure of the calculated composition to match the K_2O and Na_2O of the samples: a) samples 78 and 79 are not related to group 52 by fractionation of the same melt, or b) samples 78 and 79 do represent the more fractionated material erupted before group 52 and comagmatic with it, but hydrothermal alteration has enriched the Na_2O and K_2O content of the rock, possibly along microfractures. Hydrothermal alteration has affected the entire base of the section of Seljavellir. (The pillow breccias were too altered for analysis of them to be useful.) Thin section examination showed that all iron oxides in sample 79 were altered, possibly to leucoxene.

Sample 62, from the dike at Seljavellir, which cuts altered hyaloclastites, is even more altered than 78 and 79. Unlike 78 and 79, it is much lower in Na_2O and K_2O than the calculated rock derived from either proposed parent. If alteration is to be blamed in this case, it must have leached the original rock.

The next two erupted compositions chronologically (group 51, 55, 56 and sample 60) can easily be derived from the composition of 52, as can be seen from Table VII. The next two compositions (59 and 67, and flow 57) can be derived from either parent composition, 81 or the 52 group.

The post-glacial flows at Seljavellir cannot be derived from parent composition 52, but only from 81. It may be significant that a tillite separates these post-glacial flows from the rest of the sequence at Seljavellir.

The other basaltic composition which can be derived by fractionating 52 as a parent and which cannot be derived from 81 is the kubbaberg group 84 and 95 from Sydstamörk. This is more difficult to explain because 84, 95 overlies 81 (after an interval of moberg formation and erosion). It is possible that the lack of a complete exposed section has resulted in a misinterpretation of the stratigraphy and that 81 and 82 really are later flows which broke through the lower moberg or flowed along the edge of the mountain between it and the glacier. This explanation would allow 81 to be a more recent magma which fractionated to produce the most recent flows at Seljavellir (discussed above) and at Sydstamörk (discussed below). Otherwise it must be that 81 was erupted, and the next eruption in the Sydstamörk area (not including ash) produced 84 and 95 from the same parent (52) as had produced most of the Seljavellir rocks up to that time.

The calculations show that the composition of 84, 95 can easily be used as a parent to derive both 83, a dike which cuts 84, 95, and 93, the 56% SiO_2 cinders which may be from the 1821-23 eruption.

The remainder of the Sydstamörk rocks can be derived more or less easily from the composition of 81. Late glacial and post-glacial 99, 100; 88 (Kambagils lava group), and the recent flows all have compositions in close agreement with their calculated counterparts. Sample 89, the Raudahraun, is lower in Na_2O and K_2O than the calculated residual liquid. As their name (red lava) indicates, these rocks have been thoroughly oxidized and altered and the low Na_2O and K_2O values are believed to be a result of leaching of the cinders. This sample also falls conspicuously below the trend on the Na_2O vs. SiO_2 diagram (Fig. 5).

Samples 90 and 91 at Sydstamörk, like 37 at Seljalands, are high in Na_2O and K_2O compared to other samples of similar silica content. Samples 90 and 91 are best modeled by fractionating the composition of 81, while the composition of 37 is most closely approximated by fractionating the composition of 52. Neither derivation is completely convincing, though the 52→37 calculation produces an agreement twice as good as for the 81→90 calculation. It is believed these high alkali rocks are not, in fact, related to either parent and are derived from an unknown source.

Samples 2 and 30, the nearly 55% SiO_2 cinder blocks from Seljalands, can be derived from either proposed parent composition, 81 or 52. This is also the case for samples 59 and 67, believed to be from the same eruption, as previously mentioned. The other samples of similar SiO_2 content, 108 and 109, 113, are divided between parents, sample 108 being best approximated by fractionating 81, and 109, 113 being most successfully derived from 52. The calculated composition for 109, 113 exceeds the acceptable difference limit for K_2O. This, however, could be a result of the calculated plagioclase not containing any K_2O, while the actual plagioclase precipitating out during the later stages of fractionation certainly did contain some K_2O (see plagioclase analyses in Table VI), possibly enough to bring the calculated product significantly closer to the actual composition of 109, 113.

Use of ferro-augite as a fractionating phase to form the 55% silica rocks is considered justified, as similar augites are observed in sample 2. Samples 59, 67, 108, 109, and 113 are all extremely fine grained and contain very few phenocrysts, all plagioclase.

The most difficult compositions to derive using this model are the silicic ones from the moraines. This is to be expected as they are the farthest removed from any starting "parent" composition.

The composition of sample 77, believed to be a fragment of composite dike, can be derived only from sample 52. The calculated derived composition is very similar to the sample composition. It requires 75% crystallization of a parent the composition of 52 (which, as seen from the AFM diagram, Fig. 8, must already be the residual liquid of a crystallization process). This is not believed to be a problem, however, because of the extremely small volume of acid rocks on Eyjafjöll and the close association of acid and more mafic rocks. (Blebs of quenched basalt are ubiquitous in the silicic rocks sampled.) Two of the frequently-mentioned objections to deriving acid rocks by fractionating basalts can therefore be discounted. The necessary volume of mafic composition crystallized at some depth and never seen is not overwhelming. Later mafic melts can be called upon to mobilize the small volumes of silica-rich residual melt. The occurrence of one of the most silicic rocks as a composite dike, and the blebs of quenched basalt within the silicic rocks support this proposed mechanism. (For further discussion of coexisting acid and mafic rocks, see Walker, 1963; Walker and Skelhorn, 1966; and Yoder, 1973.)

Group 107, 110, and 112 (66.81% SiO_2), like sample 77, can be most nearly approximated by fractionating parent composition 52. This provides a calculated composition considerably higher in both Na_2O and K_2O than the observed rock, but it is the closest composition obtained to the 107 group. Whether this difference in alkalis is significant, or simply exists because the group is altered, is not known. (107 is so clouded with alteration that it is not possible to focus the thin section; 110 is much fresher, but not free of alteration.) It is also possible that the K_2O difference results from use of a calculated plagioclase containing no K_2O component, whereas the plagioclase analyzed in sample 110 contained 1.11 weight % K_2O. As was mentioned in the discussion of precision and accuracy, the SiO_2 and Na_2O determinations for the high silica rocks (107, 110, 11, and 112) may not be accurate because they were above the range of the standards. It is therefore possible that the apparent excess of Na_2O in the calculated rock results simply because the analyzed Na_2O content in the rock appears lower than is actually the case.

The composition of sample 111 is best matched by a derivative of the composition of samples 2 and 30. It is interesting that it is this sample (64.92% SiO_2) which often falls off the trend on the variation diagrams (Fig. 5). This is the only sample which represents a composition derived from 2-30.

It should be realized that the solutions provided in Table VII are not unique, but depend upon the choice of compositions for the subtracted phases as well as that of the parent. Since, with the exception of plagioclase, the compositions are those of phenocrysts actually observed in the rocks, however, it is believed that the equations are reasonable approximations of what may actually be happening prior to eruption of the magmas.

Figure 11. Schematic diagram of proposed fractionation. Amount of crystallization needed to produce residual composition is shown in italics. Calculations for which $\Sigma x^2 > .1$ are shown as dashed lines.

Schematic Diagram of Proposed Fractionation

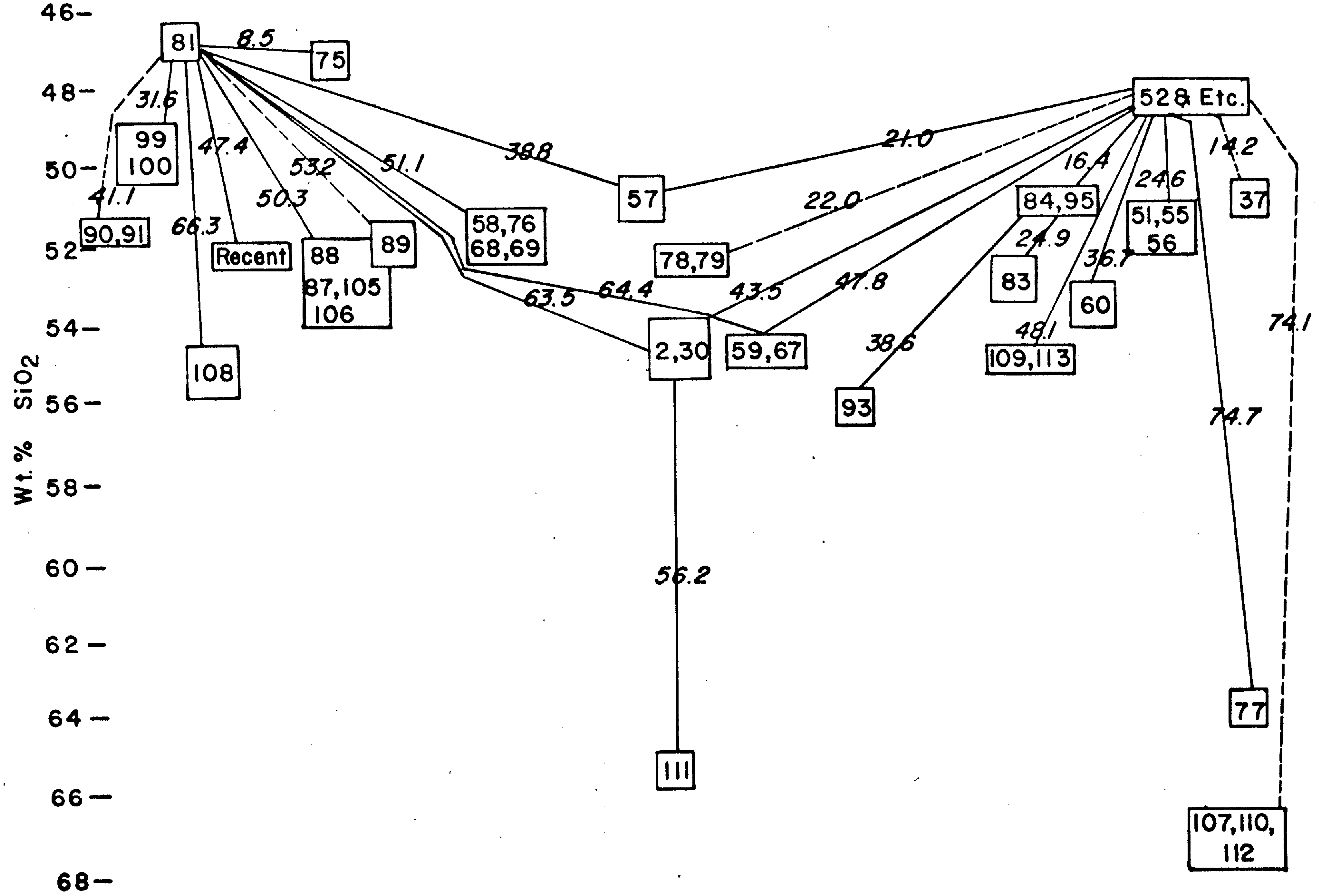

TABLE VII. FRACTIONATION MODEL CALCULATIONS

	52 etc.	- plagioclase (An 100)	- cpx (82)	- ol (78)	- mt (53)	- ilm (82)	= calculated	78,79
	128.17%	8.57%	12.14%	0%	6.11%	1.35%		
SiO_2	48.60	43.20	50.21	39.43	.05	.02	52.50	52.36
Al_2O_3	15.27	36.64	4.00	0	4.76	.14	15.66	15.61
FeO^1	13.08		7.91	19.83	66.07	44.07	11.17	11.07
MgO	4.54		14.52	42.12	5.19	1.63	3.72	3.75
CaO	9.29	20.16	21.23	.23	0	0	7.61	7.51
Na_2O	3.45		.43	0	0	0	4.38	4.47
K_2O	.95		0	0	0	0	1.22	1.50*
TiO_2	3.43		1.44	0	17.51	50.81	2.47	2.40*
							98.73	98.67
								$\Sigma x^2 = .14^2$

	52 etc.	- plagioclase (An 38)	- cpx (82)	- ol (78)	- mt (53)	- ilm (82)	= calculated	62
	139.02%	25.23%	5.11%	0%	7.89%	.79%		
SiO_2	48.60	58.93	50.21	39.43	.05	.02	50.13	49.94
Al_2O_3	15.27	26.05	4.00	0	4.76	.14	14.08	13.95
FeO^1	13.08		7.91	19.83	66.07	44.07	12.22	12.06
MgO	4.54		14.52	42.12	5.19	1.63	5.15	5.06
CaO	9.29	7.74	21.23	.23	0	0	9.88	9.73
Na_2O	3.45	7.28	.43	0	0	0	2.94	2.49*
K_2O	.95		0	0	0	0	1.33	.85*
TiO_2	3.43		1.44	0	17.51	50.81	2.92	2.79
							98.65	96.87
								$\Sigma x^2 = .56^2$

TABLE VII. (cont.)

	52 etc. -	plagioclase (An 72) -	cpx (82) -	ol (78) -	mt (53) -	ilm (82) =	calculated	51,55
	132.58%	13.89%	11.71%	.37%	5.22%	1.39%		
SiO_2	48.60	50.39	50.21	39.43	.05	.02	51.41	51.39
Al_2O_3	15.27	31.80	4.00	0	4.76	.14	15.11	15.10
FeO^1	13.08		7.91	19.83	66.07	44.07	12.29	12.27
MgO	4.54		14.52	42.12	5.19	1.63	3.87	3.86
CaO	9.29	14.49	21.23	.23	0	0	7.82	7.81
Na_2O	3.45	3.33	.43	0	0	0	4.07	4.06
K_2O	.95		0	0	0	0	1.26	1.27
TiO_2	3.43		1.44	0	17.51	50.81	2.76	2.75
							98.59	98.51

$\Sigma x^2 = <.01^2$

	52 etc. -	plagioclase (An 73) -	cpx (82) -	ol (82) -	mt (53) -	ilm (82) =	calculated	60
	158.04%	23.59%	21.59%	1.05%	9.27%	2.54%		
SiO_2	48.60	49.98	50.21	38.66	.05	.02	53.77	53.72
Al_2O_3	15.27	32.08	4.00	0	4.76	.14	15.26	15.23
FeO^1	13.08		7.91	22.47	66.07	44.07	11.49	11.45
MgO	4.54		14.52	39.88	5.19	1.63	3.10	3.08
CaO	9.29	14.81	21.23	.42	0	0	6.60	6.58
Na_2O	3.45	3.14	.43	0	0	0	4.62	4.64
K_2O	.95		0	0	0	0	1.51	1.57
TiO_2	3.43		1.44	0	17.51	50.81	2.20	2.17
							98.55	98.44

$\Sigma x^2 = 0.1^2$

TABLE VII. (cont.)

52 etc. - plag (An 63) - cpx (82) - ol (78) - mt (53) - ilm (82) = calculated 57

	126.54%	11.64%	9.12%	.12%	3.96%	1.70%		
SiO_2	48.60	52.59	50.21	39.43	.05	.02	50.76	50.71
Al_2O_3	15.27	30.32	4.00	0	4.76	.14	15.25	15.21
FeO[1]	13.08		7.91	19.83	66.07	44.07	12.44	12.40
MgO	4.54		14.52	42.12	5.19	1.63	4.14	4.11
CaO	9.29	12.75	21.23	.23	0	0	8.34	8.31
Na_2O	3.45	4.35	.43	0	0	0	3.83	3.75
K_2O	.95		0	0	0	0	1.21	1.13
TiO_2	3.43		1.44	0	17.51	50.81	2.65	2.62
							98.62	98.24

$\Sigma x^2 = .02$[2]

52 etc. - plag (An 72) - cpx (82) - cpx (110) - ol (78) - mt (53) - ilm (82) = calculated 59,67

	191.75%	40.23%	10.24%	19.70%	7.81%	7.29%	6.48%		
SiO_2	48.60	50.35	50.21	49.52	39.43	.05	.02	54.96	54.94
Al_2O_3	15.27	31.82	4.00	.71	0	4.76	.14	15.58	15.56
FeO[1]	13.08		7.91	21.27	19.83	66.07	44.07	10.86	10.84
MgO	4.54		14.52	6.25	42.12	5.19	1.63	2.22	2.20
CaO	9.29	14.51	21.23	19.49	.23	0	0	5.95	5.93
Na_2O	3.45	3.31	.43	.44	0	0	0	5.16	5.09
K_2O	.95		0	0	0	0	0	1.83	1.74*
TiO_2	3.43		1.44	.33	0	17.51	50.81	1.80	1.78
								98.36	98.08

$\Sigma x^2 = .02$[2]

TABLE VII. (cont.)

	52	- plag (4)	- cpx (82)	- cpx (110)	- ol (78)	- mt (53)	- ilm (82)	= calc.	2,30
	177.12%	36.04%	5.80%	14.86%	8.47%	5.58%	6.37%		
SiO_2	48.60	48.50	50.21	49.52	39.43	.05	.02	54.99	54.98
Al_2O_3	15.27	31.93	4.00	.71	0	4.76	.14	14.93	14.92
FeO[1]	13.08	.65	7.91	21.27	19.83	66.07	44.07	11.14	11.13
MgO	4.54	.09	14.52	6.25	42.12	5.19	1.63	2.28	2.27
CaO	9.29	16.84	21.23	19.49	.23	0	0	6.24	6.23
Na_2O	3.45	2.46	.43	.44	0	0	0	5.14	5.07
K_2O	.95	.07	0	0	0	0	0	1.66	1.66
TiO_2	3.43	.06	1.44	.33	0	17.51	50.81	1.71	1.70
								98.09	97.96

$\Sigma x^2 = .01$[2]

	52	- plag (An 58)	- cpx (82)	- cpx (110)	- ol (78)	- mt (53)	- ilm (82)	= calc.	109,113
	292.62%	40.76%	32.25%		1.29%	15.67%	2.65%		
SiO_2	48.60	54.02	50.21		39.43	.05	.02	54.89	54.78
Al_2O_3	15.27	29.35	4.00		0	4.76	.14	15.41	15.34
FeO[1]	13.08		7.91		19.83	66.07	44.07	10.87	10.79
MgO	4.54		14.52		42.12	5.19	1.63	2.67	2.61
CaO	9.29	11.62	21.23		.23	0	0	6.31	6.25
Na_2O	3.45	5.01	.43		0	0	0	4.47	4.34
K_2O	.95		0		0	0	0	1.84	1.72*
TiO_2	3.43		1.44		0	17.51	50.81	2.06	1.99
								98.52	97.82

$\Sigma x^2 = .07$[2]

TABLE VII. (cont.)

	52 etc.	- plagioclase (4)	- cpx (82)	- ol (78)	- mt (53)	- ilm (82)	= calculated	84,95
	119.56%	9.16 %	5.38%	0%	3.61%	1.41%		
SiO_2	48.60	48.50	50.21	39.43	.05	.02	50.97	50.95
Al_2O_3	15.27	31.93	4.00	0	4.76	.14	14.95	14.97
FeO^1	13.08	.65	7.91	19.83	66.07	44.07	12.15	12.13
MgO	4.54	.09	14.52	42.12	5.19	1.63	4.43	4.50
CaO	9.29	16.84	21.23	.23	0	0	8.43	8.38
Na_2O	3.45	2.46	.43	0	0	0	3.88	3.84
K_2O	.95	.07	0	0	0	0	1.13	1.13
TiO_2	3.43	.06	1.44	0	17.51	50.81	2.67	2.67
							98.61	98.57
								$\Sigma x^2 = .01^2$

	81 etc.	- plagioclase (4)	- cpx (82)	- ol (78)	- mt (53)	- ilm (82)	= calculated	99,100
	146.24%	23.47%	14.64%	1.16%	6.97%	0%		
SiO_2	46.83	48.50	50.21	39.43	.05	.02	49.30	49.36
Al_2O_3	15.75	31.93	4.00	0	4.76	.14	14.63	14.67
FeO^1	13.30	.65	7.91	19.83	66.07	44.07	13.31	13.33
MgO	5.39	.09	14.52	42.12	5.19	1.63	4.89	4.93
CaO	10.90	16.84	21.23	.23	0	0	8.88	8.91
Na_2O	2.75	2.46	.43	0	0	0	3.39	3.44
K_2O	.63	.07	0	0	0	0	.91	.93
TiO_2	3.15	.06	1.44	0	17.51	50.81	3.17	3.29
							98.48	98.86
								$\Sigma x^2 = .03^2$

TABLE VII. (cont.)

52 etc. - plagioclase (4) (110) - cpx (82) - cpx (110) - ol (78) - mt (53) - ilm (82) = calculated 77

	52 etc.	plagioclase (4)	plagioclase (110)	cpx (82)	cpx (110)	ol (78)	mt (53)	ilm (82)	calculated	77
	395.60%	86.92%	61.91%	74.72%	9.13%	8.28%	48.18%	6.46%		
SiO_2	48.60	48.50	66.06	50.21	49.52	39.43	.05	.02	63.88	63.88
Al_2O_3	15.27	31.93	21.20	4.00	.71	0	4.76	.14	14.19	14.17
FeO^1	13.08	.65	.26	7.91	21.27	19.83	66.07	44.07	6.85	6.83
MgO	4.54	.09	0	14.52	6.25	42.12	5.19	1.63	.36	.36
CaO	9.29	16.84	2.45	21.23	19.49	.23	0	0	2.93	2.93
Na_2O	3.45	2.46	9.61	.43	.44	0	0	0	5.20	5.18
K_2O	.95	.07	1.11	0	0	0	0	0	3.01	2.94
TiO_2	3.43	.06	1.00	1.44	.33	0	17.51	50.81	.69	.63
									97.11	96.92

$\Sigma x^2 = .01^2$

52 etc. - plag (An 58) - cpx (82) - cpx (110) - ol (78) - mt (53) - ilm (82) = calculated 107

	52 etc.	plag (An 58)	cpx (82)	cpx (110)	ol (78)	mt (53)	ilm (82)	calculated	107
	386.65%	136.22%	63.17%	24.14%	9.95%	45.57%	7.60%		
SiO_2	48.60	53.89	50.21	49.52	39.43	.05	.02	66.90	66.81
Al_2O_3	15.27	29.44	4.00	.71	0	4.76	.14	14.06	14.00
FeO^1	13.08		7.91	21.27	19.83	66.07	44.07	5.01	4.95
MgO	4.54		14.52	6.25	42.12	5.19	1.63	.19	.14
CaO	9.29	11.73	21.23	19.49	.23	0	0	1.81	1.75
Na_2O	3.45	4.95	.43	.44	0	0	0	6.23	5.96*
K_2O	.95		0	0	0	0	0	3.68	3.33*
TiO_2	3.43		1.44	.33	0	17.51	50.81	.44	.38
								98.32	97.32

$\Sigma x^2 = .22^2$

TABLE VII. (cont.)

	81	- plag (4)	- cpx (82)	- ol (78)	- mt (53)	- ilm (82)	= calculated	52 etc.
	136.42%	16.96%	12.54%	1.67%	5.25%	0		
SiO_2	46.83	48.50	50.21	39.43	.05	.02	48.71	48.60
Al_2O_3	15.75	31.93	4.00	0	4.76	.14	15.33	15.27
FeO^1	13.30	.65	7.91	19.83	66.07	44.07	13.24	13.08
MgO	5.39	.09	14.52	42.12	5.19	1.63	4.54	4.54
CaO	10.90	16.84	21.23	.23	0	0	9.35	9.29
Na_2O	2.75	2.46	.43	0	0	0	3.29	3.45*
K_2O	.63	.07	0	0	0	0	.85	.95
TiO_2	3.15	.06	1.44	0	17.51	50.81	3.19	3.43*
							98.50	98.61
								$\Sigma x^2 = .12^2$

	81	- plag (An 62)	- cpx (82)	- ol (78)	- mt (53)	- ilm (82)	= calculated	62
	172.32%	38.50%	18.98%	1.53%	13.31%	0		
SiO_2	46.83	52.83	50.21	39.43	.05	.02	50.22	49.94
Al_2O_3	15.75	30.15	4.00	0	4.76	.14	14.14	13.95
FeO^1	13.30		7.91	19.83	66.07	44.07	12.32	12.06
MgO	5.39		14.52	42.13	5.19	1.63	5.20	5.06
CaO	10.90	12.56	21.23	.23	0	0	9.92	9.73
Na_2O	2.75	4.46	.43	0	0	0	2.95	2.49
K_2O	.63		0	0	0	0	1.09	.85
TiO_2	3.15		1.44	0	17.51	50.81	2.83	2.79
							98.67	96.87
								$\Sigma x^2 = .51^2$

TABLE VII. (cont.)

	81 etc.	- plagioclase (An 69)	- cpx (82)	- ol (78)	- mt (53)	- ilm (82)	= calculated	88
	201.13%	44.79%	36.16%	1.99%	17.41%	.78%		
SiO_2	46.83	51.22	50.21	39.43	.05	.02	52.31	52.26
Al_2O_3	15.75	31.24	4.00	0	4.76	.14	15.42	15.38
FeO^1	13.30		7.91	19.83	66.07	44.07	11.65	11.61
MgO	5.39		14.52	42.12	5.19	1.63	3.84	3.81
CaO	10.90	13.83	21.23	.23			8.05	8.02
Na_2O	2.75	3.71	.43	0			3.72	3.64
K_2O	.63		0	0			1.27	1.20
TiO_2	3.15		1.44	0	17.51	50.81	2.37	2.34
							98.63	98.26

$\Sigma x^2 = .02^2$

	81 etc.	- plagioclase (An 64)	- cpx (82)	- ol (78)	- mt (53)	- ilm (82)	= calculated	89
	213.83%	49.58%	43.12%	1.36%	19.05%	.72%		
SiO_2	46.83	52.42	50.21	39.43	.05	.02	51.96	51.87
Al_2O_3	15.75	30.43	4.00	0	4.76	.14	15.96	15.89
FeO^1	13.30		7.91	19.83	66.07	44.07	11.86	11.78
MgO	5.39		14.52	42.12	5.19	1.63	3.69	3.63
CaO	10.90	12.89	21.23	.23			7.77	7.69
Na_2O	2.75	4.27	.43	0			3.59	3.25*
K_2O	.63		0	0			1.35	.88*
TiO_2	3.15		1.44	0	17.51	50.81	2.41	2.35
							98.59	97.34

$\Sigma x^2 = .38^2$

TABLE VII. (cont.)

	81 etc.	- plagioclase (An 73)	- cpx (82)	- ol (78)	- mt (53)	- ilm (82)	= calculated	"recent"
	190.21%	39.76%	33.05%	1.27%	15.82%	.31%		
SiO_2	46.83	49.98	50.21	39.43	.05	.02	52.11	52.06
Al_2O_3	15.75	32.08	4.00	0	4.76	.14	15.13	15.10
FeO^1	13.30		7.91	19.83	66.07	44.07	11.85	11.81
MgO	5.39		14.52	42.12	5.19	1.63	4.10	4.07
CaO	10.90	14.81	21.23	.23			7.83	7.80
Na_2O	2.75	3.14	.43	0			3.85	3.79
K_2O	.63		0	0			1.20	1.17
TiO_2	3.15		1.44	0	17.51	50.81	2.59	2.56
							98.66	98.36
								$\Sigma x^2 = .01^2$

	81 etc.	- plagioclase (An 60)	- cpx (82)	- ol (78)	- mt (53)	- ilm (82)	= calculated	75
	109.23%	2.23%	4.41%	1.40%	1.19%	0		
SiO_2	46.83	53.39	50.21	39.43	.05	.02	47.20	47.16
Al_2O_3	15.75	29.78	4.00	0	4.76	.14	16.31	16.28
FeO^1	13.30		7.91	19.83	66.07	44.07	13.12	13.05
MgO	5.39		14.52	42.12	5.19	1.63	4.60	4.58
CaO	10.90	12.11	21.23	.23			10.70	10.66
Na_2O	2.75	4.72	.43	0			2.88	2.72*
K_2O	.63		0	0			.69	.57*
TiO_2	3.15		1.44	0	17.51	50.81	3.17	3.24
							98.67	98.26
								$\Sigma x^2 = .05^2$

TABLE VII. (cont.)

	81 etc.	- plagioclase (4)	- cpx (82)	- ol (78)	- mt (53)	- ilm (82)	= calculated	57
	163.37%	28.57%	21.88%	2.20%	9.92%	.80%		
SiO_2	46.83	48.50	50.21	39.43	.05	.02	50.80	50.71
Al_2O_3	15.75	31.93	4.00	0	4.76	.14	15.27	15.21
FeO[1]	13.30	.65	7.91	19.83	66.07	44.07	12.47	12.40
MgO	5.39	.09	14.52	42.12	5.19	1.63	4.15	4.11
CaO	10.90	16.84	21.23	.23	0	0	8.35	8.31
Na_2O	2.75	2.46	.43	0	0	0	3.70	3.75
K_2O	.63	.07	0	0	0	0	1.01	1.13
TiO_2	3.15	.06	1.44	0	17.51	50.81	2.67	2.62
							98.42	98.24

$\Sigma x^2 = .04^2$

	81 etc.	- plagioclase (An75)	- cpx (82)	- ol (78)	- mt (53)	- ilm (82)	= calculated	58,76
	204.41%	48.93%	35.49%	4.53%	13.90%	1.56%		
SiO_2	46.83	49.57	50.21	39.43	.05	.02	51.87	51.76
Al_2O_3	15.75	32.35	4.00	0	4.76	.14	14.29	14.22
FeO[1]	13.30		7.91	19.83	66.07	44.07	13.61	13.53
MgO	5.39		14.52	42.12	5.19	1.63	3.21	3.16
CaO	10.90	15.13	21.23	.23	0	0	7.34	7.28
Na_2O	2.75	2.95	.43	0	0	0	4.03	3.96
K_2O	.63		0	0	0	0	1.29	1.32
TiO_2	3.15		1.44	0	17.51	50.81	2.70	2.64
							98.34	97.87

$\Sigma x^2 = .04^2$

TABLE VII. (cont.)

	84,95 -	plag (An 64) -	cpx (82) -	cpx (110) -	ol (78) -	mt (53) -	ilm (82) =	calculated	83
	133.16%	14.95%	10.86%	0	2.80%	4.14%	.41%		
SiO_2	50.95	52.37	50.21	49.52	39.43	.05	.02	53.47	53.37
Al_2O_3	14.97	30.46	4.00	.71	0	4.76	.14	14.75	14.69
FeO[1]	12.13		7.91	21.27	19.83	66.07	44.07	11.82	11.75
MgO	4.50		14.52	6.25	42.12	5.19	1.63	3.02	2.97
CaO	8.38	12.92	21.23	19.49	.23	0	0	6.92	6.87
Na_2O	3.84	4.25	.43	.44	0	0	0	4.44	4.40
K_2O	1.13		0	0	0	0	0	1.51	1.52
TiO_2	2.67		1.44	.33	0	17.51	50.81	2.47	2.41
								98.40	97.99

$\Sigma x^2 = .03^2$

	84,95 -	plag (An 70) -	cpx (82) -	cpx (110) -	ol (82) -	mt (53) -	ilm (82) =	calculated	93
	162.94%	27.38%	12.79%	7.42%	6.53%	6.00%	2.82%		
SiO_2	50.95	50.81	50.21	49.52	38.66	.05	.02	56.49	56.47
Al_2O_3	14.97	31.51	4.00	.71	0	4.76	.14	14.91	14.90
FeO[1]	12.13		7.91	21.27	22.47	66.07	44.07	10.51	10.49
MgO	4.50		14.52	6.20	39.88	5.19	1.63	2.05	2.04
CaO	8.38	14.14	21.23	19.49	.42	0	0	5.60	5.58
Na_2O	3.84	3.52	.43	.44	0	0	0	5.21	5.16
K_2O	1.13		0	0	0	0	0	1.85	1.78
TiO_2	2.67		1.44	.33	0	17.51	50.81	1.66	1.65
								98.28	98.07

$\Sigma x^2 = .01^2$

TABLE VII. (cont.)

	81 -	plag (An 77) -	cpx (82) -	cpx (110) -	ol (78) -	mt (53) -	ilm (82) =	calculated	2,30
	273.62%	81.05%	17.19%	37.25%	16.12%	13.92%	8.06%		
SiO_2	46.83	48.99	50.21	49.52	39.43	.05	.02	55.00	54.98
Al_2O_3	15.75	32.74	4.00	.71	0	4.76	.14	14.94	14.92
FeO^1	13.30		7.91	21.27	19.83	66.07	44.07	11.15	11.13
MgO	5.39		14.52	6.25	42.12	5.19	1.63	2.28	2.27
CaO	10.90	15.59	21.23	19.49	.23	0	0	6.25	6.23
Na_2O	2.75	2.68	.43	.44	0	0	0	5.12	5.07
K_2O	.63		0	0	0	0	0	1.73	1.66
TiO_2	3.15		1.44	.33	0	17.51	50.81	1.71	1.70
								98.18	97.96

$\Sigma x^2 = .01^2$

	81 -	plag (An 76) -	cpx (82) -	cpx (110) -	ol (78) -	mt (53) -	ilm (82) =	calculated	59,67
	281.10%	82.64%	21.13%	38.70%	15.52%	15.33%	7.78%		
SiO_2	46.83	49.36	50.21	49.52	39.43	.05	.02	54.95	54.94
Al_2O_3	15.75	32.49	4.00	.71	0	4.76	.14	15.57	15.56
FeO^1	13.30		7.91	21.27	19.83	66.07	44.07	10.85	10.84
MgO	5.39		14.52	6.25	42.12	5.19	1.63	2.21	2.20
CaO	10.90	15.30	21.23	19.49	.23	0	0	5.94	5.93
Na_2O	2.75	2.85	.43	.44	0	0	0	5.12	5.09
K_2O	.63		0	0	0	0	0	1.78	1.74
TiO_2	3.15		1.44	.33	0	17.51	50.81	1.79	1.78
								98.21	98.08

$\Sigma x^2 = <.01^2$

TABLE VII. (cont.)

	2,30	- plag (An 35)	- cpx (93)	- cpx (110)	- ol (78)	- mt (53)	- ilm (82)	= calculated	111
	228.50%	66.64%	22.50%	17.86%	2.93%	18.37%	.20%		
SiO_2	54.98	59.68	50.23	49.52	39.43	.05	.02	64.82	64.92
Al_2O_3	14.92	25.54	1.37	.71	0	4.76	.14	15.76	15.81
FeO[1]	11.13		13.43	21.27	19.83	66.07	44.07	4.57	4.58
MgO	2.27		12.60	6.25	42.12	5.19	1.63	.16	.20
CaO	6.23	7.15	19.41	19.49	.23	0	0	1.63	1.63
Na_2O	5.07	7.63	.36	.44	0	0	0	6.34	6.23
K_2O	1.66		0	0	0	0	0	3.79	3.77
TiO_2	1.70		.60	.33	0	17.51	50.81	.36	.43
								97.43	97.57

$\Sigma x^2 = .03^2$

	81	- plag (An 73)	- cpx (82)	- cpx (93)	- cpx (110)	- ol (78)	- mt (53)	- ilm (82)	= calculated	108
	296.77%	90.68%	19.39%	3.38%	42.25%	15.42%	18.22%	7.43%		
SiO_2	46.83	50.21	50.21	50.23	49.52	39.43	.05	.02	55.02	55.01
Al_2O_3	15.75	31.92	4.00	1.37	.71	0	4.76	.14	15.81	15.80
FeO[1]	13.30		7.91	13.43	21.27	19.83	66.07	44.07	10.13	10.12
MgO	5.39		14.52	12.60	6.25	42.12	5.19	1.63	2.56	2.55
CaO	10.90	14.63	21.23	19.41	19.49	.23	0	0	6.05	6.04
Na_2O	2.75	3.24	.43	.36	.44	0	0	0	4.95	4.94
K_2O	.63		0	0	0	0	0	0	1.88	1.87
TiO_2	3.15		1.44	.60	.33	0	17.51	50.81	1.95	1.94
									98.35	98.27

$\Sigma x^2 = <.01^2$

TABLE VII. (cont.)

	81	- plag (An 100)	- cpx (82)	- cpx (93)	- ol (82)	- mt (53)	- ilm (82)	= calculated	90,91
	169.81%	28.68	0	26.89	4.57	7.72	1.95		
SiO_2	46.83	43.20	50.21	50.23	38.66	.05	.02	51.86	51.73
Al_2O_3	15.75	34.64	4.00	1.37	0	4.76	.14	15.50	15.43
FeO^1	13.30		7.91	13.43	22.47	66.07	44.07	11.99	11.90
MgO	5.39		14.52	12.60	39.88	5.19	1.63	3.51	3.47
CaO	10.90	20.16	21.23	19.41	.42	0	0	7.49	7.46
Na_2O	2.75		.43	.36	0	0	0	4.58	4.89*
K_2O	.63		0	0	0	0	0	1.07	1.37*
TiO_2	3.15		1.44	.60	0	17.51	50.81	2.85	2.78
								98.85	99.03

$\Sigma x^2 = .22^2$

	52	- plag (An 100)	- cpx (82)	- cpx (93)	- ol (78)	- mt (53)	- ilm (82)	= calculated	37
	116.51%	5.59	6.42	0	0	3.98	.52		
SiO_2	48.60	43.20	50.21	50.23	39.43	.05	.02	50.99	50.91
Al_2O_3	15.27	36.64	4.00	1.37	0	4.76	.14	15.30	15.32
FeO^1	13.08		7.91	13.43	19.83	66.07	44.07	11.87	11.81
MgO	4.54		14.52	12.60	42.12	5.19	1.63	4.15	4.27*
CaO	9.29	20.16	21.23	19.41	.23	0	0	8.34	8.25
Na_2O	3.45		.43	.36	0	0	0	4.00	4.26*
K_2O	.95		0	0	0	0	0	1.11	1.21
TiO_2	3.43		1.44	.60	0	17.51	50.81	2.95	2.92
								98.71	98.95

$\Sigma x^2 = .11^2$

TABLE VII. (cont.)

[1] Total Fe_2O_3 as FeO.

[2] Σx^2 equals the sum of the squares of the differences for all oxides.

* See text.

CONCLUSIONS

The calculations in Table VII demonstrate that nearly all the compositions of the Eyjafjöll rocks which were analyzed can be related to one of two parental magmas by fractionating out plagioclase, clinopyroxene, magnetite, ilmenite, and usually minor amounts of olivine. The fact that so little olivine is removed to derive the more silicic rocks does not imply that not much olivine crystallizes from the basalts. Olivine phenocrysts are found in all the basalts.

I have chosen to represent (Fig. 10, Table VII) the fractionation process as starting with the compositions of 82 or the 52 group, with the understanding that these were not primary compositions, but represent a minimum amount of fractionation. The AFM diagram (Fig. 8) reveals that most of the olivine crystallization has taken place between the primary composition and the "parental" compositions designated in this paper. What distinguishes the "parental" compositions from the more differentiated compositions is not much additional olivine crystallization, but the crystallization and subtraction of plagioclase, clinopyroxene, and magnetite, with or without ilmenite.

It is possible that the two "parental" magmas are related by fractionation to a single primary composition, never seen on the surface. It is demonstrated, however, that most of the rock compositions found on Eyjafjöll can be derived convincingly from only one of the "parent" compositions, and that (with an apparent exception at Sydstamörk, where 81 is found below 84, 95) the family of 52 and its products is the earlier, while the products of 81 are late or post-glacial.

Mass balance calculations for the major elements lead to two principal conclusions about the rocks of Eyjafjöll. One is that the silicic rocks can be derived from the basalts by a fractionation process; neither a separate source nor a re-melting of older solidified basalts is required to generate the Na_2O and K_2O contents observed. The second is that there may have been a change in the composition of the parent magmas with time. If indeed there are two separate parental magmas, the earlier one, represented by the composition of the 52 group, appears to be richer in alkalis and TiO_2 than the later one, represented by 81. This hypothesis is supported by the plot of the various compositions on the alkali vs. silica diagram (Figure 6). As previously mentioned, it is the most recent flows which plot on the tholeiitic side of the Hawaiian dividing line.

Future trace element studies of the Eyjafjöll rocks are planned to test the genetic relationships proposed in the present work.

Another potentially interesting subject for future research would be a comparison of the compositions of basalts and basaltic-andesites from previous cycles on Hekla, to see whether there has been any systematic change in alkali content or degree of silica saturation with time.

ACKNOWLEDGEMENTS

I would like to thank my advisor, Prof. John S. Dickey, Jr., for his encouragement and guidance during the writing of this thesis; Mary Roden, who did all the drafting; and Ellen Loiselle, who typed the manuscript. I also must thank the family at Sydstamörk for their hospitality, Margrét Kjartansdottir for her untiring help and encouragement with the field work, Danielle Chouet for her translation from the German of Thoroddsen's work on Eyjafjallajökull, John Ludden for computerization of the mass absorption corrections for the XRF data, and Marc Loiselle for performing the replicate XRF analyses at WHOI.

The University of Iceland and the Nordic Volcanological Institute were most gracious in permitting use of their analytical and field equipment. Special thanks go to Carla Montgomery for her patient editorial assistance.

Financial support for the author while in Iceland, and for the field work, was provided by the Fulbright Foundation and the Icelandic Government. Partial funding for microprobe analyses came from NSF Grants 75-21848 EAR and 76-03766 EAR to S.R. Hart (MIT). Additional funds for further microprobe work, for computer time, and some thesis preparation costs were provided by the Department of Earth and Planetary Sciences, MIT.

REFERENCES

Albee, A.L. and L. Ray, 1970. Correction factors for electron probe microanalysis of silicates, oxides, carbonates, phosphates, and sulfates. Anal. Chem., 42:1408-1414.

Baldridge, W.S., T.R. McGetchin, F.A. Frey, and E. Jarosewich, 1973. Magmatic evolution of Hekla, Iceland. Contrib. Mineral. Petrol., 42:245-258.

Bence, A.E. and A.L. Albee, 1968. Empirical correction factors for the electron microanalysis of silicates and oxides. J. Geol., 76:382-403.

Carswell, D.A., 1978. Jökull, in press.

Carmichael, I.S., 1964. The petrology of Thingmuli, a Tertiary volcano in eastern Iceland. J. Petrol., 5:435-460.

Doherty, P.C. and T.L. Wright, 1971. Mineral distribution program Mod. II (for solving petrologic mixing problems), Geol. Surv. Computer Contrib. No. 7, open file report, U.S.G.S. Computer Center Division, Menlo Park.

Einarsson, Th., 1968. Jardfraedi. Reykjavik, Mál og Menning, 335 p.

Finger, L.W. and L. Hadadiacos, 1972. Electron microprobe automation. Carnegie Inst. Wash. Yearbook, 71:598-600.

Harvey, P.K., D.M. Taylor, R.D. Hendry, and F. Bancroft, 1973. An accurate fusion method for the analysis of rocks and chemically related materials by X-ray fluorescence spectrometry. X-Ray Spectrometry, 3:33-44.

Jakobsson, S.P., 1972. Chemistry and distribution pattern of Recent basaltic rocks in Iceland. Lithos, 5:365-386.

Justus, P.S., 1978. Systematic curvi-columnar jointing in First Watchung Mountain Basalt, N.J.: reinterpretation of origin and significance. Geol. Soc. Amer. Abs. with Programs, 10:49.

Kjartansson, G., 1958. Endaslepp hraun undir Eyjafjöllum. Náttúrufraedingurinn, 28:129-140.

MacDonald, G.A. and T. Katsura, 1964. Chemical composition of Hawaiian lavas. J. Petrol., 5:82-133.

Rose, H.J., Jr., I. Adler, and F.J. Flanagan, 1963. X-ray fluorescence analysis of the light elements in rocks and minerals. Appl. Spectr., 17:81-85.

Saemundsson, K., 1970. Interglacial lava flows in the lowlands of southern Iceland and the problem of two-tiered columnar jointing. Jökull, 20:62-77.

Sigvaldason, G.E., 1974. The petrology of Hekla and origin of silicic rocks in Iceland. in The Eruption of Hekla, 1947-1948, V,1, Reykjavik Vísindafélag Islendinga, 44 p.

Thorarinsson, S., 1975. Geology and physical geography. In Iceland, 874-1974, Reykjavik, Central Bank of Iceland, 1-32.

Thorarinsson, S., 1975. Katla og annáll Kötlugosa. Árbók Ferdafélags Islands, 125-149.

Thorarinsson, S., S. Steinthorsson, Th. Einarsson, H. Kristmannsdottir, and N. Oskarsson, 1973. The eruption on Heimaey, Iceland. Nature, 241:372-375.

Thoroddsen, Th., 1925. Die geschichte der Isländischen vulkane. Copenhagen, Det Konelige Danske Videnskebernes Selskabs, 141-143.

Van Bemmelen, R.W. and M.G. Rutten, 1955. Table Mountains of Northern Iceland. Leiden, E.J. Brill, 217 p.

Walker, G.P.L., 1963. The Breiddalur central volcano, eastern Iceland. Quart. J. Geol. Soc., London, 119: 29-63.

Walker, G.P.L. and R.R. Skelhorn, 1966. Some associations of acid and basic igneous rocks. Earth Sci. Rev., 2:93-109.

Watkins, N.D., 1972. Review of the development of the geomagnetic polarity time scale and discussion of prospects for its finer definition. Geol. Soc. Amer. Bull., 83:551-574.

Wilkinson, J.F.G., 1967. Petrography of basaltic rocks. In Hess, H.H. and A. Poldervaart (eds.), The Poldervaart Treatise on Rocks of Basaltic Composition, Vo. 1, New York, Interscience, 163-214.

Yoder, H.S., Jr., 1973. Contemporaneous basaltic and rhyolitic magmas. Amer. Mineral., 58:153-171.